ACS Infectious Diseases

pubs.acs.org/journal/aidcbc

Review

Current and Perspective Diagnostic Techniques for COVID-19

Xi Yuan,[†] Chengming Yang,[†] Qian He, Junhu Chen, Dongmei Yu, Jie Li, Shiyao Zhai, Zhifeng Qin, Ke Du,* Zhenhai Chu,* and Peiwu Qin*

Cite This: *ACS Infect. Dis.* 2020, 6, 1998−2016

Read Online

ACCESS | Metrics & More | Article Recommendations

ABSTRACT: Since late December 2019, the coronavirus pandemic (COVID-19; previously known as 2019-nCoV) caused by the severe acute respiratory syndrome coronavirus 2 (SARS-CoV-2) has been surging rapidly around the world. With more than 1,700,000 confirmed cases, the world faces an unprecedented economic, social, and health impact. The early, rapid, sensitive, and accurate diagnosis of viral infection provides rapid responses for public health surveillance, prevention, and control of contagious diffusion. More than 30% of the confirmed cases are asymptomatic, and the high false-negative rate (FNR) of a single assay requires the development of novel diagnostic techniques, combinative approaches, sampling from different locations, and consecutive detection. The recurrence of discharged patients indicates the need for long-term monitoring and tracking. Diagnostic and therapeutic methods are evolving with a deeper understanding of virus pathology and the potential for relapse. In this Review, a comprehensive summary and comparison of different SARS-CoV-2 diagnostic methods are provided for researchers and clinicians to develop appropriate strategies for the timely and effective detection of SARS-CoV-2. The survey of current biosensors and diagnostic devices for viral nucleic acids, proteins, and particles and chest tomography will provide insight into the development of novel perspective techniques for the diagnosis of COVID-19.

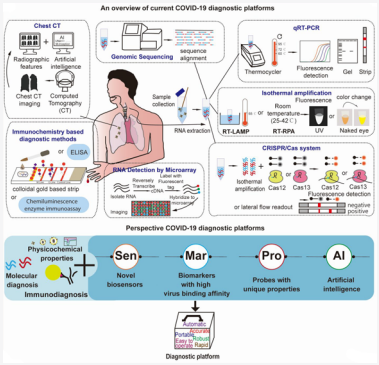

KEYWORDS: *COVID-19, SARS-CoV-2, diagnostics, biosensors, molecular diagnostics, immunoassay*

The rapid increase in confirmed cases of COVID-19 remains uncontrollable, with an increase of approximately 200,000 diagnosed patients globally per day. So far, according to the WHO official counts, this widespread outbreak of coronavirus has over 1,700,000 infected cases with more than 670,000 deaths.[1] SARS-CoV-2 is the pathogen that causes COVID-19. SARS-CoV-2 is named because of its genetic similarity to the severe acute respiratory syndrome coronavirus 1 (SARS-CoV-1) discovered in 2003. Belonging to the coronavirus (CoVs) clade, SARS-CoV-2 has a single-stranded positive-sense RNA genome with 30 kilobases in length and is about 80−120 nm in diameter.[2] SARS-CoV-2 is the seventh CoVs known to cause infections in humans. Of the six previously discovered coronaviruses, four of them (HCoV-OC43, -229E, -NL63, and -HKU1) caused common cold symptoms in immunocompetent individuals,[3] while the remaining two (SARS-CoV-1 and MERS-CoV) had high mortality rates of zoonotic origin.[4]

Early symptoms in COVID-19 patients include fever, dry cough, shortness of breath, headache, muscle soreness, and fatigue.[5,6] However, the symptoms are not deterministic due to the identification of asymptomatic SARS-CoV-2 carriers and the overlapping features with other acute respiratory viral infections such as influenza.[5−7] Therefore, highly sensitive and specific diagnostic methods that can distinguish COVID-19 cases from healthy or other virus-infected individuals are essential for disease management and therapeutics. Currently, various organizations have reported a variety of methods for the clinical diagnosis of COVID-19, which have different principles, operations, costs, and sensitivities. Here, we thoroughly review current diagnostic techniques for researchers and clinicians to develop appropriate methods for the timely and effective diagnosis of COVID-19 or the detection of SARS-CoV-2. The principles learned from other viral diagnostics will guide the SARS-CoV-2 diagnostics development. The review of other viral particle, nucleic acid, and protein detection methods provides insight into the development of novel SARS-CoV-2 diagnostic techniques.

■ SARS-CoV-2

In the early stage of the COVID-19 outbreak in Wuhan, researchers isolated the virus from infected pneumonia patients and characterized the pathogen using metagenomic next-generation sequencing (mNGS) and electron microscopy.[8,9]

Received: May 29, 2020
Published: July 17, 2020

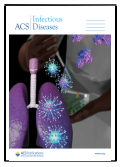

SARS-CoV-2 is a pathological nanoparticle composed essentially of protein and RNA. The first draft of the SARS-CoV-2 genome was released on January 10, 2020 (GenBank: MN908947). The SARS-CoV-2 genome is 29,891 nucleotides in length, encoding 9,860 amino acids that are homologous to lineage B β-CoVs.[8,10,11] SARS-CoV-2 is 96.3% homologous to BatCoV RaTG13 but discordant with SARS-CoV-1 and MERS-CoV.[12]

The SARS-CoV-2 genome contains five major open reading frames (ORFs), arranged in the order of the 5′ untranslated region (UTR)-replicase complex (ORF1ab)-Spike (S)-Envelope (E)-Membrane (M)-Nucleocapsid (N)-3′ UTR and accessory genes such as **3a**, **6**, **7a**, **7b**, and **8** (Figure 1).[8,10]

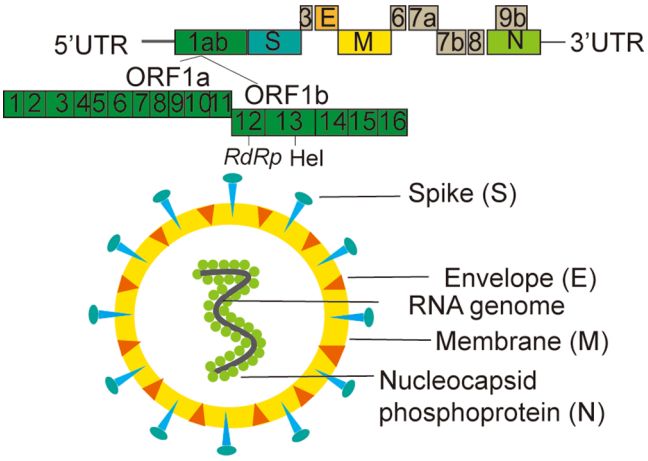

Figure 1. SARS-CoV-2 genomic organization and virus structure.

The ORF1ab gene encodes the nonstructural proteins that aid viral genome replication and transcription, which has about 90% nucleotide sequence (nts) identity to SARS-CoV-1.[11] The E gene, which encodes the membrane protein involving virus assembly, budding, envelop formation, and pathogenesis,[13] has the highest (93%) nts identity with SARS-CoV-1. The S gene, responsible for virus binding and cell entry,[14] shares less than 75% nts identity with other SARS-CoVs, except for RaTG13 (93%).[11] Compared to S and E proteins, M and N proteins are more abundant, which bind to the RNA genome and participate in virus assembly and budding, respectively, where the M and N genes share approximately 90% nts identity with SARS-CoV-1.[11]

SARS-CoV-2 infection is initiated with viral entry, in which the S protein first recognizes and binds to angiotensin-converting enzyme 2 (ACE2), a host membrane receptor, and then induces fusion of the virus membrane with the host cell membrane.[8] The next step is the entry of the virion or its RNA genome. The viral antigen is then presented by the antigen-presenting cells, which subsequently stimulates humoral and cellular immunity. The primary humoral immune response has a typical pattern of IgA, IgM, and IgG production. IgG antibodies are primarily S- and N-specific antibodies,[15] which can be utilized as antigens for SARS-CoV-2 antibody development.

■ DIAGNOSTIC APPROACHES TO COVID-19

Diagnosis of COVID-19 by Viral Cytopathic Effects. According to the Koch's postulates, virus isolation from clinical samples remains the "gold standard" for diagnosing viral infections. The enriched virus minimizes the perturbation from the patients' samples and increases the signal-to-noise ratio for virus detection. Nasopharyngeal swab (NPS), oropharyngeal swab (OPS), bronchoalveolar lavage fluid (BALF), sputum, and stool samples collected from suspicious cases are used for virus isolation.[16] Sampling operations, specimen source, and sampling time all affect diagnosis to a certain extent.[17] The extracted virus shows obvious cytopathogenic effects in both Vero and Huh7 cells, resulting in observable morphological changes visualized by electron microscopy after nucleocapsid staining.[8] A TMPRSS2-expressing VeroE6 cell line is highly susceptible to SARS-CoV-2 infection, making it ideal for virus isolation and cytopathic testing.[18] Photoclickable fluorogenic probes enable the visualization of specific DNA or RNA with precise spatiotemporal control in their native cellular environment,[19] facilitating the diagnosis of the viral cytopathic effect. However, virus isolation and visualization are impractical for large-scale diagnosis of COVID-19, since SARS-CoV-2 requires at least 3 days to inflict obvious cytopathic effects on selected cell lines.[8] In addition, virus isolation and culture require well-trained personnel and a Biosafety Level 3 environment, which are not available in most healthcare clinics.[20]

Detection of SARS-CoV-2 Intact Particles. The assimilated principles from other virus diagnostic techniques lay a solid foundation for the development of novel diagnostic techniques for SARS-CoV-2. A portable platform captures viruses by their sizes, coupled with Raman spectroscopy for identification.[21] The SARS-CoV-2 particles in aerosol can be characterized with on-chip spectroscopy using a photonic cavity enhanced silicon nitride (Si_3N_4) racetrack resonator-based sensor.[22] The electrochemical biosensor based on surface imprinted polymers and graphene oxide composites can identify isolated virus, which has a limit of detection (LoD) similar to RT-PCR for Zika virus detection.[23] Solid-state micro- and nanopores monitor viral particles in the air by cross-pore ionic current.[24] Capillary biosensor, which is employed for the detection of bacterial and viral pathogens, uses a multicolumn capillary for easy separation, Fe nanoclusters for signal amplification, and a smartphone for image analysis.[25] After capturing the virus, microbeads generate a unique diffraction pattern of "blurry beads" on a smartphone.[26] The smartphone-based colorimetric assay utilizes 3D nanostructures as a scaffold for conjugating antibodies to capture virus particles, where the 3D structure provides more virus binding sites.[27] DNA origami-based aptasensors for virus, viral RNA, and protein detection need further attention due to their 3D structure, simple fabrication, and rapid response.[28] Interdigitated organic electrochemical transistors function as transducers to enhance the sensitivity and dynamic detection range of aptasensors.[29] Moreover, a viral imprinted polymer-based biosensor detects the virus at ng/mL.[30] An ultrasensitive electrolyte-gated field-effect transistor (FET) transduces biorecognition events into virus concentrations.[31] Lab-on-a-chip having a specific biosensor and sensitive detector is desirable for SARS-CoV-2 diagnostics without nucleic acid isolation and amplification.[32]

Direct Detection of SARS-CoV-2 RNA. Detection techniques for mRNA or miRNA can be adapted for the detection of SARS-CoV-2 RNA. The miRNA logic sensing techniques amplify signal gain with a programmed nanoparticle network, which is composed of DNA-bridged gold nanoparticles and quantum dots (QDs).[33] Chemiluminescence with

https://dx.doi.org/10.1021/acsinfecdis.0c00365
ACS Infect. Dis. 2020, 6, 1998−2016

Table 1. Published SARS-CoV-2 Diagnosis Methods

S/N	method	target	testing sample source	LoD[a]	specificity	time	instrument
1	qRT-PCR[147]	E and RdRp gene	RNA transcripts	E gene: 3.9 copies/reaction; RdRp gene: 3.6 copies/reaction	RdRP-P2 probe is specific to SARS-CoV-2; E gene assay is not specific to SARS-CoV-2	2–4 h	real-time PCR system
2	qRT-PCR[148]	RdRp/helicase (Hel), S, and N gene	RNA transcripts	RdRp/Hel gene: 11.2 copies/reaction; N gene: 21.3 copies/reaction	RdRp/Hel gene assay with no cross-reaction with other coronaviruses, but the RdRp-P2 assay cross-reacts with SARS-CoV-1 culture lysate	2–4 h	real-time PCR system
3	qRT-PCR[149]	ORF1b and N gene	ORF1b and N gene cloned into plasmids	10 copies/reaction	specific to Sarbecoviruses	2–4 h	real-time PCR system
4	RT-LAMP[150]	A fragment (2941-3420) of GenBank MN908947	synthetic ssDNA	1.02 fg/reaction	no cross-reaction with other coronaviruses	45 min	UV and temperature control equipment
5	iLACO (RT-LAMP)[63]	ORF1ab gene	synthetic RNA	10 copies/reaction	not mentioned	15–40 min	temperature control equipment
6	fluorescent closed-tube Penn-RAMP[79]	ORF1ab gene	synthetic DNA	7 copies/reaction	not mentioned	75 min	BioRad Thermal Cycler
			mimic sample[b]	100% sensitivity at 7 virions/reaction	not mentioned		
	colorimetric closed-tube Penn-RAMP[79]	ORF1ab gene	synthetic DNA	100 targets/reaction	not mentioned		temperature control equipment
7	RPA/SHERLOCK assay[83]	S and ORF1ab gene	synthetic RNA	10 copies/μL	not mentioned	1 h	water bath and microcentrifuge
8	RT-LAMP/Cas12 DETECTR assay[84]	E and N gene	synthetic RNA	10 copies/μL	no cross-reaction with other coronaviruses	40 min	temperature control equipment
9	antisense oligonucleotide capped plasmonic nanoparticles[151]	N gene	viral RNA from the cellular lysate	180 ng/mL	not mentioned	10 min	temperature control equipment
10	dual-functional plasmonic photothermal (PPT) enhanced LSPR biosensing system[152]	RdRp, ORF1ab, and E gene	synthetic DNA	0.22 pM	not mentioned	several minutes	dual-functional plasmonic PPT enhanced LSPR biosensing system, spectrometer

[a]LoD is the lowest concentration of analyte that is detected (≥95%). [b]Mimic sample: spiked the swabs with various concentrations of pathogens.

https://dx.doi.org/10.1021/acsinfecdis.0c00365
ACS Infect. Dis. 2020, 6, 1998−2016

Table 2. Information about Diagnostic Kits for SARS-CoV-2 Approved by US FDA for Emergency Use[58]

S/N	test kit	principle	technique	molecular targets	specimen	instrument	LoD and specificity	time	remarks
1	1 copy COVID-19 qPCR Multi Kit	molecular	qRT-PCR	E and RdRP gene	upper respiratory specimen	real-time PCR instrument	200 copies/mL; E gene cross-reacts with other SARS-CoV	not mentioned	
2	Alinity m SARS-CoV-2 assay	molecular	qRT-PCR	RdRp and N gene	nasal swabs, OPS, NPS, and BALF	Alinity m system	100 copies/mL; no cross-reactivity	not mentioned	
3	Gnomegen COVID-19-RT-qPCR Detection Kit	molecular	qRT-PCR	N gene	NPS and OPS	Applied Biosystems Real-time PCR system 7500 (ABI 7500)	10 copies/reaction; no cross-reactivity	not mentioned	
4	Rutgers Clinical Genomics Laboratory TaqPath SARS-CoV-2-Assay	molecular	qRT-PCR	N, S, and ORF1ab gene	upper and lower respiratory tract fluids	real-time PCR instrument	200 copies/mL; cross-reacts with some organisms	not mentioned	
5	Quick SARS-CoV-2rRT-PCR Kit	molecular	qRT-PCR	N gene	upper and lower respiratory specimens	CFX96 Touch Real-Time PCR Detection System	83 genomic equivalents copies (GEC)/mL; cross-reacts with some organisms	not mentioned	
6	OPTI SARS-CoV-2 RT PCR Test	molecular	qRT-PCR	N gene	upper and lower respiratory specimens	ABI 7500	700 copies/mL in sputum and 900 copies/mL in NPS; no cross-reactivity	not mentioned	
7	SARS-CoV-2 R-GENE	molecular	qRT-PCR	N, RdRP, and E gene	upper respiratory specimens and BALF	real-time PCR instrument	0.43 TCID50/mL[a]; no cross-reactivity	not mentioned	
8	FTD SARS-CoV-2	molecular	qRT-PCR	N and ORF1ab gene	upper respiratory specimens and BALF	real-time PCR instrument	2.3×10^{-3} TCID50/mL; no cross-reactivity	not mentioned	
9	Novel Coronavirus (2019-nCoV) Nucleic Acid Diagnostic Kit (PCR-Fluorescence Probing)	molecular	qRT-PCR	ORF1ab and N genes	upper respiratory specimens	ABI 7500	200 copies/mL; no cross reactivity	not mentioned	
10	Bio-Rad SARS-CoV-2 ddPCR Test	molecular	qRT-PCR	N gene	upper respiratory specimens	Bio-Rad C1000 Touch or S1000 thermocyclers	625 copies/mL; no cross reactivity	not mentioned	
11	LabGun COVID-19 RT-PCR Kit	molecular	qRT-PCR	RdRP and N gene	upper respiratory specimens	real-time PCR instrument	2×10^4 copies/mL; cross-reacts with SARS-CoV-1	not mentioned	
12	Rheonix COVID-19 MDx Assay	molecular	qRT-PCR	N gene	upper respiratory specimens and BALF	Rheonix Encompass MDx Workstation	625 copies/mL; cross-reacts with some organisms	not mentioned	fully automatic operation
13	U-TOP COVID-19 Detection Kit	molecular	qRT-PCR	ORF1ab and N genes	upper respiratory specimens	real-time PCR instrument	1×10^3 copies/mL; no cross reactivity	not mentioned	
14	STANDARD M nCoV Real-Time Detection Kit	molecular	qRT-PCR	RdRp and E gene	upper respiratory specimens and sputum	real-time PCR instrument	250 and 125 copies/mL for upper and lower respiratory specimens, respectively; cross-reacts with SARS-CoV-1.	not mentioned	
15	RealStar SARS-CoV02 RT-PCR Kits U.S.	molecular	qRT-PCR	S and E gene	upper respiratory specimens	CFX96 Systems	0.1 pfu/mL; no cross-reactivity	not mentioned	
16	Allplex 2019-nCoV Assay	molecular	qRT-PCR	E, RdRP, and N gene	upper and lower respiratory specimens	CFX96 Systems	1.25×10^3 copies/mL; no cross-reactivity	not mentioned	
17	PhoenixDx 2019-CoV	molecular	qRT-PCR	RdRp and E gene	NPS, OPS, nasal swab, and BALF	BIO-RAD CFX96-IVD platform	100 copies/mL; no cross-reactivity except E gene target	not mentioned	
18	GeneFinder COVID-19 Plus RealAmp Kit	molecular	qRT-PCR	RdRp, N, and E gene	upper respiratory, BALF, and sputum specimens	real-time PCR instrument	500 copies/mL; no cross-reactivity except E gene target	not mentioned	
19	Fosun COVID-19 RT-PCR Detection Kit	molecular	qRT-PCR	ORF1ab, N, and E gene	upper and lower respiratory specimens	real-time PCR instrument	300 copies/mL; no cross-reactivity	not mentioned	
20	Curative-Korva SARS-Cov-2 Assay	molecular	qRT-PCR	N gene	OPS, NPS, nasal swab, and oral fluid	real-time PCR instrument	200 copies/mL; no cross-reactivity	not mentioned	

https://dx.doi.org/10.1021/acsinfecdis.0c00365
ACS Infect. Dis. 2020, 6, 1998−2016

Table 2. continued

S/N	test kit	principle	technique	molecular targets	specimen	instrument	LoD and specificity	time	remarks
21	GS COVID-19 RT-PCR KIT	molecular	qRT-PCR	OFR1ab, E, and N gene	upper respiratory specimens	ABI 7500	1×10^3 copies/mL; cross-reacts with some organisms	not mentioned	
22	SARS-CoV-2 Fluorescent PCR Kit	molecular	qRT-PCR	N and E gene	upper respiratory specimens	ABI 7500	1×10^3 copies/mL; cross-reacts with SARS-CoV-1	not mentioned	
23	QuantiVirus SARS-CoV-2 Test Kit	molecular	qRT-PCR	N, ORF1ab, and E genes	upper respiratory specimens and sputum	real-time PCR instrument	200 copies/mL; no cross reactivity	not mentioned	
24	BD SARS-CoV-2Reagents for BD MAX System	molecular	qRT-PCR	N gene	nasal swab, NPS, and OPS	BD MAX System	40 genomic equivalents (GE)/mL; no cross reactivity	not mentioned	
25	Smart Detect SARS-CoV-2 rRT-PCR Kit	molecular	qRT-PCR	RdRp, N, and E gene	upper respiratory specimens	ABI 7500	1.1×10^4 GE/mL; no cross reactivity	not mentioned	
26	Logix Smart Coronavirus Disease 2019 (COVID-19) Kit	molecular	qRT-PCR	COVID-19 specific RNA	lower and upper respiratory tract fluids	real-time PCR instrument	4.29×10^3 copies/mL; no cross-reactivity	not mentioned	
27	ScienCell SARS-CoV-2 Coronavirus Real-time RT-PCR (RT-qPCR) Detection Kit	molecular	qRT-PCR	N1, N2, and RP gene	nasal swab, NPS, OPS, and BALF	LightCycler 96 Real-Time PCR System	103.5 copies/mL; no cross-reactivity	not mentioned	
28	ARIES SARS-CoV-2 Assay	molecular	qRT-PCR	ORF1ab and N gene	NPS	Luminex ARIES Systems	7.5×10^4 copies/mL; no cross-reactivity	2 h	fully automatic operation
29	BioGX SARS-CoV-2 Reagents for BD MAX System	molecular	qRT-PCR	N1 and N2 genes	NPS and OPS	BD MAX System and BD MAX Sample RackAm	40 copies/mL; no cross-reactivity	not mentioned	
30	COV-19 IDx Assay	molecular	qRT-PCR	N and RP genes	NPS and OPS	KingFisher Flex nucleic acid extraction systems and Applied Biosystems QuantStudio12 Flex	8.5×10^3 copies/mL; no cross-reactivity	not mentioned	
31	QIAstat-Dx Respiratory SARS-CoV-2 Panel	molecular	qRT-PCR	ORF1b poly and E gene	NPS	QIAstat Dx Analyzer System	500 copies/mL; no cross-reactivity	about 1 h	fully automatic operation
32	NeuMoDx SARS-CoV-2 Assay	molecular	qRT-PCR	Nsp2 and N gene	upper respiratory specimens	NeuMoDx 288 Molecular System or NeuMoDx 96 Molecular System	150 copies/mL; no cross-reactivity	about 1 h	fully automatic operation
33	NxTAG CoV Extended Panel Assay	molecular	qRT-PCR	ORF1ab, N, and E gene	NPS	Luminex instrument; computer; thermal cyclers; end-point thermal cycler	5×10^3 GCE/mL; no cross-reactivity	2−3 h	
34	Real-Time Fluorescent RT-PCR Kit for Detecting SARS-CoV-2	molecular	qRT-PCR	ORF1ab gene	throat swabs and BALF	ABI 7500	100 copies/mL; no cross-reactivity	not mentioned	
35	AvellinoCoV2 test	molecular	qRT-PCR	N gene	NPS and OPS	ABI 7500	5.5×10^4 copies/mL; no cross-reactivity	not mentioned	testing is limited to Avellino Lab USA
36	PerkinElmer New Coronavirus Nucleic Acid Detection Kit	molecular	qRT-PCR	N and ORF1ab gene	OPS and NPS	PerkinElmer PreNAT II Automated Workstation; ABI 7500	N gene: 24.884 copies/mL; ORF1ab gene: 9.307 copies/mL; no cross-reactivity	not mentioned	
37	Xpert Xpress SARS-CoV-2 Test	molecular	qRT-PCR	N and E gene	NPS, nasal wash, and aspirate specimens	GeneXpert Xpress System	250 copies/mL; no cross-reactivity	not mentioned	fully automatic operation
38	Primerdesign Ltd. COVID-19 genesig Real-Time PCR Assay	molecular	qRT-PCR	ORF1ab gene	OPS	real-time PCR instrument	330 copies/mL; no cross-reactivity	not mentioned	
39	Simplexa COVID-19 Direct Assay	molecular	qRT-PCR	ORF1ab and S gene	NPS	LIAISON MDX instrument	500 copies/mL; cross-reacts with SARS-coronavirus	not mentioned	no sample extraction is needed

https://dx.doi.org/10.1021/acsinfecdis.0c00365
ACS Infect. Dis. 2020, 6, 1998−2016

Table 2. continued

S/N	test kit	principle	technique	molecular targets	specimen	instrument	LoD and specificity	time	remarks
40	Abbott RealTime SARS-CoV-2 Assay	molecular	qRT-PCR	RdRp and N gene	NPS and OPS	Abbott m2000sp and Abbott m2000rt instruments	100 virus copies/mL; no cross-reactivity	not mentioned	a total of 96 samples can be processed in each run
41	Quest SARS-CoV-2 rRT-PCR	molecular	qRT-PCR	N gene	upper and lower respiratory specimens	ABI 7500; MagNA Pure 96 Instrument	136 copies/mL; no cross-reactivity	not mentioned	
42	Lyra SARS-CoV-2 Assay	molecular	qRT-PCR	nonstructural polyprotein (pp1ab)	NPS and OPS	ABI 7500	800 copies/mL; no cross-reactivity	not mentioned	
43	COVID-19 RT-PCR Test	molecular	qRT-PCR	N gene	upper and lower respiratory specimens	ABI 7500	6.25×10^3 copies/mL; N3 target cross-reacts with SARS-like viruses	not mentioned	
44	Panther Fusion SARS-CoV-2 Assay	molecular	qRT-PCR	ORF1ab gene	NPS and OPS	Panther Fusion System	1×10^{-2} TCID50/mL; no cross-reactivity	not mentioned	automatic amplification, detection, and data reduction
45	TaqPath COVID-19 Combo Kit	molecular	qRT-PCR	ORF1ab, N, and S gene	NPS, OPS, and BALF	ABI 7500	10 copies/reaction; no cross-reactivity	not mentioned	
46	cobas SARS-CoV-2	molecular	qRT-PCR	ORF1/a and E gene	NPS and OPS	Cobas 6800/8800 Systems	0.9×10^{-2} TCID50/mL; no cross-reactivity	within 3.5 h	fully automatic operation
47	New York SARS-CoV-2 Real-time Reverse Transcriptase (RT)-PCR Diagnostic Panel	molecular	qRT-PCR	N gene	NPS, OPS, and sputa	ABI 7500	25 copies/reaction; no cross-reactivity	not mentioned	
48	CDC 2019-nCoV Real-Time RT-PCR Diagnostic Panel (CDC)	molecular	qRT-PCR	N gene	upper and lower respiratory specimens	ABI 7500	1×10^3 copies/mL; no cross-reactivity	not mentioned	
49	Gnomegen COVID-19 RT-Digital PCR Detection Kit	molecular	qRT-digital PCR	N1, N2, and RP gene	nasal swab, NPS, and OPS	QuantStudioTM 3D Digital PCR System; thermocycler	8 copies/reaction; no cross-reactivity	not mentioned	
50	BioFire Respiratory Panel 2.1 (RP2.1)	molecular	nested RT-PCR	S and M gene	NPS	FilmArray system	500 copies/mL; cross-reacts with some organisms	45 min	fully automatic operation
51	BioFire COVID-19 Test	molecular	nested RT-PCR	ORF1ab and ORF8 gene	NPS	FilmArray 2.0/Torch Instrument Systems and FilmArray Pouch Loading Station	330 copies/mL; no cross-reactivity	50 min	fully automatic operation
52	Sherlock CRISPR SARS-CoV-2 Kit	molecular	CRISPR/Cas system	ORF1ab and N gene	upper respiratory specimens and BALF	heat block and microplate reader	ORF1ab gene: 6.75×10^3 copies/mL; N target: 1.35×10^3; no cross-reactivity	1 h	
53	iAMP COVID-19 Detection Kit	molecular	isothermal amplification	ORF1ab and N gene	NPS and OPS	Biorad CFX96 Real-Time System	400 copies/mL; no cross-reactivity	not mentioned	
54	ID NOW COVID-19	molecular	isothermal amplification	RdRp gene	nasal, throat, or nasopharyngeal specimens	ID NOW instrument	125 copies/mL; no cross-reactivity	≤13 min	fully automatic operation; can be used outside of the clinical laboratory environment
55	Accula SARS-Cov-2 Test	molecular	use PCR to amplify the nucleic acid and read result with a detection strip	N gene	throat and nasal swabs	Accula Dock or Silaris Dock	100 copies/reaction; no cross-reactivity	30 min	can be used in patient care settings outside of the clinical laboratory environment
56	ePlex SARS-CoV-2 Test	molecular	qRT-PCR combined with electrochemical detection	not mentioned	NPS	The True Sample-to-Answer Solution ePlex instrument	1×10^5 copies/mL; cross-reacts with SARS CoV-1	not mentioned	fully automatic operation
57	Sofia 2 SARS Antigen FIA	antigen	lateral flow immunoassay	N protein	NPS and OPS	Sofia 2 instrument	Swab LoD: TCID50 1.13×10^2 /mL; cross-reacts with SARS-CoV-1	15 min	

https://dx.doi.org/10.1021/acsinfecdis.0c00365
ACS Infect. Dis. 2020, 6, 1998−2016

Table 2. continued

S/N	test kit	principle	technique	molecular targets	specimen	instrument	LoD and specificity	time	remarks
58	Anti-SARS-CoV-2 ELISA (IgG)	serology IgG	ELISA	S1 domain of the S protein	serum or plasma	automatic microplate washer; microplate reader; incubator	sensitivity is unknown; cross-reacts with Anti-SARS-CoV-1 IgG	not mentioned	
59	COVID-19 ELISA IgG Antibody Test	serology IgG	ELISA	S protein	serum and plasma	microplate reader	sensitivity is unknown; no cross-reactivity	not mentioned	tests should be performed at Mount Sinai Laboratory
60	Platelia SARS-CoV-2 Total Ab Assay	serology total antibody	ELISA	N protein	serum and plasma	dry-heat incubator; microplate washing system and microplate reader	sensitivity is unknown; cross-reaction is possible with MERS-CoV	not mentioned	
61	Elecsys Anti-SARS-CoV-2	serology antibody	electrochemiluminescence immunoassay (ECLIA)	N protein	serum and plasma	Cobas e analyzer	Sensitivity is unknown; no cross reactivity	18 min	
62	SARS-CoV-2 IgG Assay	serology IgG only	chemiluminescent microparticle immunoassay (CMIA)	N protein	serum and plasma	ARCHITECT i2000SR instrument	sensitivity is unknown; cross-reacts with some organisms	not mentioned	
63	LIAISON SARS-CoV-2 S1/S2 IgG	serology IgG only	chemiluminescent immunoassay (CLIA)	S protein	serum and plasma	LIAISON XL analyzer	sensitivity is unknown; cross-reacts with some organisms	not mentioned	
64	VITROS Immunodiagnostic Products Anti-SARS-CoV-2 IgG Reagent Pack	serology IgG only	CLIA	S protein	serum	VITROS ECi/ECiQ/3600 Immunodiagnostic Systems and the VITROS 5600/XT 7600 Integrated Systems	sensitivity is unknown; no cross-reactivity	48 min	
65	Anti-SARS-CoV-2 Rapid Test	serology IgM and IgG	lateral flow immunoassay	S protein	serum and plasma	centrifuge	sensitivity is unknown; no cross-reactivity	20 min	
66	qSARS-CoV-2 IgG/IgM Rapid Test	serology IgM and IgG	lateral flow immunoassay	SARS-CoV-2 IgG/IgM	serum, plasma, or venipuncture whole blood	no sophisticated instrument is needed	no cross-reactivity	15–20 min	
67	DPP COVID-19 IgM/IgG System	serology IgM and IgG	immunochromatographic test	N protein	fingerstick whole blood, venous whole blood, serum, or plasma samples	no sophisticated instrument is needed	sensitivity is unknown	not mentioned	
68	New York SARS-CoV Microsphere Immunoassay for Antibody Detection	serology total antibody	microsphere immunoassay	N protein	serum	Luminex FlexMap dual laser cytometer	88% at 25 days post-symptom onset; cross-reacts with some organisms	not mentioned	
69	VITROS Immunodiagnostic Products Anti-SARS-CoV-2 Total Reagent Pack	serology total antibody	immunometric	S protein	serum and plasma	VITROS ECi/ECiQ/3600 Immunodiagnostic System and the VITROS 5600/XT 7600 Integrated Systems	sensitivity is unknown; no cross-reactivity	48 min	

[a]TCID50/mL: Median tissue culture infectious dose per milliliter.

https://dx.doi.org/10.1021/acsinfecdis.0c00365
ACS Infect. Dis. 2020, 6, 1998−2016

a smartphone is capable of detecting miRNA through RNA-triggered in situ growth of nanoprobes in spherical nucleic acid enzymes, such as nanolabels and amplifiers.[34] Another miRNA biosensor uses generic neutravidin combined with electrochemically encoded responsive nanolabels to measure the opening of molecular beacons by means of a square-wave stripping voltammetry.[35] The biosensor that combines cyclic amplification with hairpin DNA detects attomolar miRNA via surface plasmon-enhanced electrochemiluminescence.[36] The gold nanoparticle with an RNA three-way junction motif can sense miRNA using electrochemical surface-enhanced Raman spectroscopy.[37] The photoelectrochemical biosensor, based on a MoS_2/g-C_3N_4/black TiO_2 heterojunction as the photoactive material and gold nanoparticles carrying Histostar antibodies for signal amplification, captures miRNA that leads to horseradish peroxidase (HRP) immobilization, whose insoluble products in the electrode reduce photocurrent.[38]

The dual signal amplification system with the hybridization chain reaction and enzyme-induced metallization with anodic stripping voltammetry measures miRNA in the femtomole range.[39] The polydiacetylene microtube waveguide with catalytic hairpin assembly as a signal amplification strategy shows femtomolar sensitivity for RNA detection.[40] The amperometric genosensor based on peptide nucleic acid (PNA) probes immobilized on carbon nanotube-screen printed electrodes determines trace levels of viral RNA.[41] The plasmonic nanoparticle-based optical biosensor array functionalized with capture DNA binds to complementary viral RNA, which can be reversed by chemical treatment (10 mM HCl).[35] FET with a two-dimensional channel made of a single graphene layer achieves label-free detection of RNA down to attomolar concentration.[42] Single-molecule fluorescence resonance energy transfer remains a promising tool for multiplex viral RNA detection (~200 pM) with interconvertible hairpin-based sensors.[43] Nanoporous anodic alumina supports oligonucleotides as gated ensembles to detect the presence of viral RNA.[44] The 3D nanostructure has a high surface-to-volume ratio and well-controlled shape factors for virus and nucleic acid capture.[45] Previously, a bead-stacked nanodevice has been developed for pathogen trapping[46] and micropillar polydimethylsiloxane, for rapid viral DNA sensing.[47] Protein nanopore detects viral RNA at the single-molecule level using specific DNA probes.[48]

Digital-resolution detection of viral RNA by photonic resonator absorption microscopy relies on RNA-activated nanoparticle−photonic crystal hybrid coupling.[49] Polyadenine-mediated spherical nucleic acid probes on gold nanoparticles facilitate the programmable detection of RNA in saliva or serum samples.[50] Carbon and graphene quantum dots have unique electronic and fluorescent properties, which can be conjugated to RNA or DNA substrate for viral RNA detection.[51] Upconversion nanoprobes with external luminescence quenchers are expected to be used for viral RNA detection due to their high energy transfer efficiency.[52] Carbon nanotube-based sensors have demonstrated the potential of viral optical detection without purification, amplification, and labeling.[53] Nanoparticles fabricated or printed on a 3D structure and functionalized with PNA or DNA efficiently capture SARS-CoV-2 RNA, where single molecule or signal amplification cascade enables the ultrasensitive label-free detection.

SARS-CoV-2 Detection with Genomic Sequencing. For an unknown virus, genomic sequencing is important for its rapid and complete identification. Genomic sequencing has many advantages in virus detection. First, it enables investigation of the SARS-CoV-2 evolution during transmission and tracking of coronavirus movements.[54] Second, sequencing can effectively exclude other pathogens. Third, genomic sequencing can identify multiple pathogens existing in a single patient, which helps implement reasonable treatments. However, operation and data analysis require expensive equipment, long turnaround time, and professional bioinformatics personnel. Droplet-based single-cell sequencing technology, such as inDrop, Drop-seq, and 10× Genomics with barcoded beads, can deliver primers to the beads and achieve high detection efficiency.[55] Currently, viral genome sequencing has top priority at the current stage of the outbreak, but patients' genome sequencing will be informative in understanding human susceptibility to SARS-CoV-2.

SARS-CoV-2 Detection with Quantitative Reverse Transcription-Polymerase Chain Reaction (qRT-PCR). Currently, qRT-PCR is commonly used for the clinical diagnosis of SARS-CoV-2 infection.[56] The steps of qRT-PCR are as follows: (1) extract RNA from patient samples; (2) reversely transcribe viral RNA into cDNA and then amplify the specific cDNA fragment by PCR; (3) read the fluorescent signal. Smaller Cycle threshold (C_t) values indicate positive diagnostic results. The C_t value of qPCR is the cycle number at which the fluorescent signal of a qPCR product rises above the background threshold.

Some qRT-PCR methods achieve single molecular sensitivity (within 10 molecules) in the laboratory (Table 1). Regarding clinical diagnosis, 11 fluorescent qRT-PCR kits have received emergency approval from China's National Medical Products Administration (NMPA),[57] and 53 qRT-PCR kits have received an Emergency Use Authorization (EUA) by the Food and Drug Administration (FDA) (Table 2).[58] These SARS-CoV-2 qRT-PCR kits targeting the S, E, N, or ORF1ab genes are a single- or multiple-target system. The PerkinElmer New Coronavirus Nucleic test kit has the lowest LoD (N gene: 24.884 copies/mL; ORF1ab gene: 9.307 copies/mL).

qRT-PCR requires a 2−4 h turnaround time and a laboratory certified under the Clinical Laboratory Improvement Amendments (CLIA) or a clinical laboratory with trained personnel, whose efficiency is low to satisfy the screening requirements of the COVID-19 pandemic. The automated qRT-PCR instrument, which integrates RNA extraction, concentration measurement, reagent preparation, and target sequence amplification/detection steps, has achieved significant improvements in detection efficiency and assay throughput (Table 2). The US FDA has approved five automated PCR-based systems that can return diagnostic results in less than an hour: the Accula SARS-CoV-2 test on Accula dock or Silaris dock (30 min), the BioFire COVID-19 test and BioFire Respiratory Panel 2.1 on the FilmArray system (50 and 45 min), the QIAstat-Dx Respiratory SARS-CoV-2 Panel on the QIAstat-Dx Analyzer System (1 h), and the NeuMoDx SARS-CoV-2 Assay on the NeuMoDx 288 Molecular System (1 h). The Accula integrates PCR with lateral flow technologies, while the ePlex combines DNA hybridization with electrochemical detection. QIAstat-Dx, and BioFire Respiratory Panel 2.1 (RP2.1) are multiplexed and can distinguish SARS-CoV-2 from other bacteria and viruses (more than 21 types). Fully automated diagnostic devices have a LoD of 125 to 1×10^5 copies/mL, which seems less sensitive than

https://dx.doi.org/10.1021/acsinfecdis.0c00365
ACS Infect. Dis. 2020, 6, 1998−2016

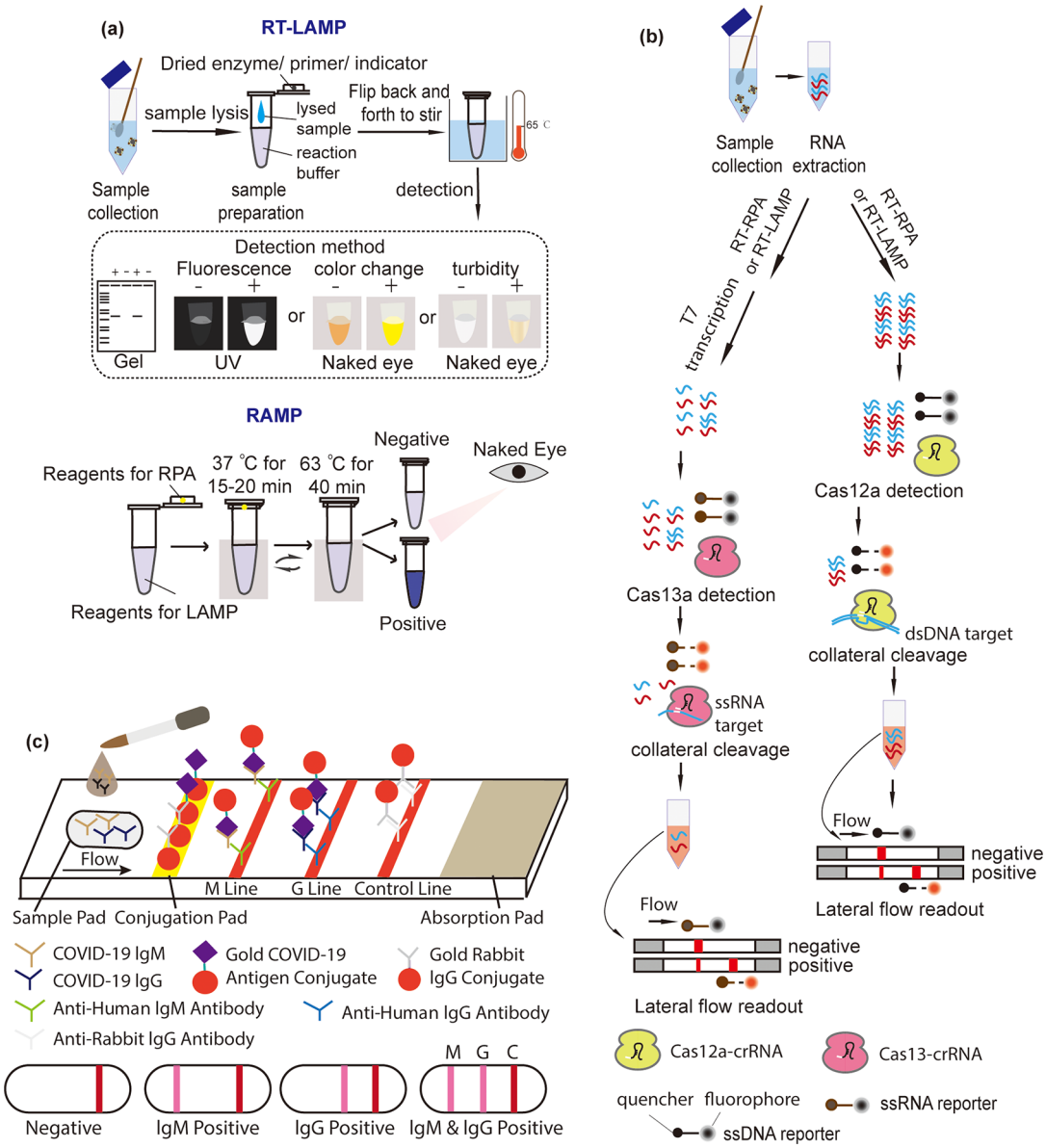

Figure 2. Schematic diagram of current diagnostic approaches of COVID-19: (a) SARS-CoV-2 RNA detection with isothermal amplification;[63,79] (b) SARS-CoV-2 RNA detection with the CRISPR-Cas system;[83,84] (c) SARS-CoV-2 IgM/IgG combined antibody test.[85]

nonfully automated diagnostic devices with a LoD of 10 to 5.5 × 10^4 copies/mL.

qRT-PCR-based diagnostic techniques have several advantages. First, it is more suitable for early stage diagnosis than the antigen−antibody reaction, since it takes time to trigger the immune response. Second, qRT-PCR can dynamically monitor the degree of viral infection and assess the prognosis. However, the COVID-19 diagnostic FNR of qRT-PCR exceeded 30%.[17,59] Some asymptomatic COVID-19 patients show abnormal manifestations on their CT images before positive qRT-PCR.[60]

Here are the possible reasons that can explain the FNR. First, the mutation leads to the off-target mismatch between the primer and the target sequence. The ORF1a, ORF 8, and N gene contain hot-spot loci such as 28 144 in ORF 8 (30.53%), 8782 in ORF1a (29.47%), and 29 095 in N (11.58%).[61] Second, for asymptomatic, mildly symptomatic, or discharged patients, low viral loads may be insufficient for qRT-PCR detection. Third, the presence of interfering substances may generate "false-positive" results. Furthermore, the conditions of specimen transportation and preservation as well as the quality of the test kits may significantly affect the diagnostic accuracy. The integration of the qRT-PCR with clinical manifestations and imaging examinations is more efficient and accurate in diagnosing suspected COVID-19 patients. Furthermore, microfluidic digital array PCR that provides gene quantification at the single-molecule level may reduce the false-positive rate.[62]

SARS-CoV-2 RNA Detection with Isothermal Amplification. Loop-mediated isothermal amplification (LAMP) for SARS-CoV-2 detection avoids the high-temperature melting step in PCR by using strand displacement DNA polymerase in conjunction with 4 to 6 specially designed primers to achieve highly specific DNA amplification, which can realize 10^9−10^{10}-fold amplification in 15−60 min at 65 °C. The one-step single-tube reverse transcription LAMP (RT-LAMP) can detect as low as 10 copies of RNA fragments within 15−40 min (Figure 2a).[63] The final amplification products can be visualized by

https://dx.doi.org/10.1021/acsinfecdis.0c00365
ACS Infect. Dis. 2020, 6, 1998−2016

agarose gel electrophoresis or real-time monitoring by fluorescence, turbidity, or colorimetry. Silicon bead-based microfluidics can detect the amplification product in the femtomolar range.[64] Nanopores fabricated in the silicon nitride membrane can quantify DNA concentration in attomoles.[65] A label-free impedimetric electrochemical biosensor identifies Zika DNA in a nanomolar range.[66] The DNA sensor based on the synergistic enhancement strategy of Zn-doped MoS_2 quantum dots and reductive Cu(I) particles determines the DNA in a nanomolar concentration.[67] Universal DNA biosensing based on electrostatic attraction between hexaammineruthenium(III) and DNA molecules detects DNA in solution without the immobilization of capture probes on the electrode. Stepping gating of ion channels on the nanoelectrode via DNA hybridization, carbon dot stabilized silver−lipid nanohybrids, and carbon nanotube-based FET shows label-free DNA detection.[68−70]

Digital LAMP on a track-etched polycarbonate membrane can quantify DNA fragments at 10 copies/μL.[71] qLAMP with bisintercalating DNA redox reporters amplifies DNA in 10 min.[72] Fractal LAMP automatically detects label-free DNA in subnanoliter droplets.[73] "LAMP-seq" combines RT-LAMP with next-generation sequencing for large-scale COVID-19 diagnostics.[74] LAMP and a graphene-based screen-printed electrochemical sensor can lead to on-site detection of the pathogen's nucleic acid.[75] The LAMP-based ID NOW system automatically returns the result in 13 min, which has a LoD of 125 copies/mL for SARS-CoV-2 detection, and has been approved by the US FDA for emergency use. The droplet microfluidic LAMP is high throughput for viral RNA detection.[76] The use of eosin photopolymerization for the detection of colorimetric LAMP products reduces false-positive risk.[77]

The recombinase polymerase amplification (RPA) uses recombinases, single-stranded DNA-binding proteins (SSB), and displacement enzymes to replace the high-temperature step in PCR. RPA achieves 10^4-fold amplification in 10 min at a temperature between 25 and 42 °C.[78] Two-stage Penn-RAMP combines LAMP with RPA for the diagnosis of COVID-19: RPA at 38 °C for 15−20 min and LAMP at 63 °C for 40 min (Figure 2b).[79] The signal readout is either fluorescent or colorimetric, which is 10 times more sensitive than LAMP and qRT-PCR for detecting SARS-CoV-2 mimics. Rolling circle amplification (RCA)-actuated LAMP measures miRNA in the attomolar range.[80] RCA-based nicking-assisted enzymatic cascade amplification captures amplicons with magnetic nanoparticles through real-time optomagnetic measurement, which can detect dengue virus at the femtomolar (fM) level.[81] Microfluidic-circular fluorescent probe-mediated isothermal amplification can detect viruses up to 10 copies/μL.[82]

With the naked eye or microphone readout, LAMP, RPA, and RCA permit the diagnosis of SARS-CoV-2 in the clinic or at home by minimally trained personnel with a simple temperature control device. However, commonly used LAMP requires a complex design of six primers with significant restrictions on their respective position and orientation. Besides, LAMP is not appropriate for multiplex detection due to primer−primer interactions. RPA is inhibited by genomic DNA (20−100 ng/μL); thus, RNA purification is required. The combination of digital, automatic, quantitative, and droplet microfluidic isothermal amplification and other techniques such CRISPR and nanotechnology represents the vigorous future research direction.

SARS-CoV-2 RNA Detection with CRISPR/Cas System. The CRISPR/Cas system, as a potent technology for genome editing,[86,87] has recently been transformed into virus detection.[88,89] Elements of this system include Cas proteins, guide RNAs (gRNAs), and target RNA/DNA fragments. Both Cas13a and Cas12a have collateral cleavage activity after target binding, where nonspecific single-stranded RNA or DNA labeled with a fluorescent reporter and quencher are digested and released, respectively (10^4-fold).[89,90] CRISPR/Cas13a combined with RPA can achieve a LoD of 10−100 copies/μL.[91] Previously, we integrated CRISPR/Cas13a with microfluidics and custom-designed a mini-fluorometer to detect Ebola virus at 20 plaque forming units (pfu)/mL.[90] The assay combining CRISPR/Cas13a with isothermal amplification for the detection of SARS-CoV-2 has been released,[83] demonstrated in clinical scenarios,[92] and approved by the US FDA for emergency use. Cas12a combined with RT-LAMP exhibits a LoD of 10 copies/μL with 90% sensitivity and 100% specificity in clinical samples.[84] We have applied the Cas12a assay to detect Africa Swine Fever Virus DNA up to 100 fM.[89] Viral RNA or transcribed cDNA passing through nanopores will generate double or triple peaks for viral nucleic acid characterization if the Cas13a or Cas12a complex is associated with the target sequence.[93] CRISPR is the RNA or DNA detection platform that can be integrated with any nucleic acid amplification systems.[83,84,91]

SARS-CoV-2 RNA Detection by Microarray. Microarray is a powerful analytical tool, which can simultaneously detect multiple targets in a single sample. A DNA microarray consists of a DNA probe array on a supporting material, where the DNA sequence and location are known to characterize unknown RNA/DNA samples. Today, microarray-based platforms can be classified into different families on the basis of the type of matrix (solid or liquid), the size and density of the probe, the method used for visualizing the hybridization results, and the relative costs. Microarray has the advantages of requiring a small sample volume, a rapid reaction in 15 min, and multiple probes per target, which are widely used in the diagnosis of respiratory tract viral infections.[94] High-performance nanoplasmonics and bioprinted microarrays can quantify label-free biomass, with a sample-to-data turnaround time of 40 min.[95] The optical path difference based on the transmission characteristics of the plasmonic gold nanohole determines the pathogen concentration. However, the paper-based microarray integrated with carbon nanodots, which is used for analyte recognition and the smartphone reader, exhibits great potential for viral RNA detection.[96] The coronavirus protein microarray harboring the SARS-CoV-2 and other coronavirus proteins can classify multiple types of infections.[97] Oligonucleotide microchips are hybridized with fluorescently labeled viral RNA, immobilized on a gel, fixed on a glass plate, and imaged by fluorescence microscopy.[98]

SARS-CoV-2 Detection by Immunochemistry. SARS-CoV-2 carries a variety of structural proteins on the surface, containing multiple epitopes for antibody or nanobody recognition.[99] There are various techniques for the detection of antigens and antibodies, where a single-shot mass spectrometry can distinguish viral subtypes.[100] A sandwich-type electrochemical immunosensor, which is used for the detection of virus-specific antigen based on a Pd nanoparticle (NP) functionalized electroactive Co-containing metal-organic

https://dx.doi.org/10.1021/acsinfecdis.0c00365
ACS Infect. Dis. 2020, 6, 1998−2016

framework (Co-MOF) for signal amplification, detects viral antigen up to 100 fg/mL.[101] An impedance-based biosensor identifies SARS-CoV-2 pathogens with an ACE2-decorated electrode via a self-assembled monolayer, while the performance usually improves after the insertion of redox-active alkanethiol.[102] A sensor array based on carbon or carbon polymer dots with antibody functionality can detect aqueous proteins at 100 nM.[103,104] Furthermore, the highly active Fe_3O_4 nanozyme amplifies the signals of the photoelectrochemical immunoassay.[105] A set of surface-enhanced Raman spectroscopy nanotags can detect multiple viral antigens through a sandwich immunoassay.[106] Moreover, 3D total internal reflection scattering defocus microscopy with wavelength-dependent transmission grating increases the spectral resolution and detects viral capsids at 820 μM.[107] In addition, the digital microfluidics platform based on electrowetting-on-dielectric separates antibody-bound microbeads for immunoassay.[108] The microfluidic method, using a monolithic disposable cartridge, facilitates hands-free saliva analysis by integrating sample pretreatment with electrophoretic immunoassays to measure viral antigens.[109] These available methods are important learning examples for developing the SARS-CoV-2 immunosensor.

Human SARS-CoV-2-specific antibody measurement is an alternative diagnostic method. IgM antibodies are detected after 5−7 days of infection, followed by IgG.[110] A colloidal gold immunochromatographic assay (GICA) strip and a peptide-based magnetic chemiluminescence enzyme immunoassay (MCLIA) are used to detect SARS-CoV-2 IgM and IgG antibodies (Figure 2c).[85,111] Compared to GICA and MCLIA, the SARS-CoV-2 IgG/IgM ELISA kits display a sensitivity of 87.3% with a longer time and more sophisticated operations.[112] Immunoassays can be digital and multiplexing for the detection of multiple SARS-CoV-2 subtypes by using a smartphone fluorescent reader. The reader utilizes an opto-electromechanical hardware that snaps at the back of a smartphone for data collection, interpretation, display, and communication.[113] The sensitivity of the immunosensor can be increased by means of a triple signal amplification strategy based on (i) carboxylic ester hydrolysis, (ii) electrochemical−chemical redox cycling, and (iii) electrochemical−enzymatic redox cycling.[114]

NMPA (8) and US FDA (12) have approved a variety of antibody-based kits, which can be used for the emergency detection of SARS-CoV-2 antibodies in human serum or plasma samples (Table 2). Besides, a test kit for detecting SARS-CoV-2 antigen in OPS and NPS samples has been approved by US FDA for emergency use. The immunological method circumvents the extraction of virus nucleic acid and shortens the detection time, which is safer. However, the immunological method is not applicable for the early diagnosis of COVID-19 due to the low antibody concentration at the beginning. Besides, antibody detection is susceptible to the presence of interfering substances (such as rheumatoid factor and nonspecific IgM) in blood samples[85,115] and antibody responses to SAR-CoV-2 in COVID-19 recovered patients. The SARS-CoV-2 antibody test kits are allowed to be used as a supplementary diagnostic method to nucleic acid test kits, but they cannot be used to confirm SARS-CoV-2 infection.

COVID-19 Diagnosis by Chest Computed Tomography (CT). COVID-19 is a fetal viral pneumonia, where breath chemical and respiratory behavior sensors may be helpful to diagnose and evaluate prognosis through a time-series readout. The chemoresistive orthogonal sensor array enables a simple and portable breath analyzer in daily settings.[116] A wireless wearable sensor on a paper substrate can continuously monitor respiratory behavior and transmit ultrasound data to a smartphone.[117] Chest CT demonstrates typical radiographic features in most patients with COVID-19, including ground-glass opacity, multifocal patchy consolidation, and/or interstitial changes with a peripheral distribution.[118] Typical CT features are visible in some patients with negative qRT-PCR results but with clinical symptoms.[17] C-reactive protein, erythrocyte sedimentation rate, and lactate dehydrogenase were positively correlated with the severity of pneumonia assessed on CT.[119] However, the limited number of radiologists is insufficient to accommodate a large number of patients in some regions. Deep learning (DL) typically extracts abstract features in CT images to segment the lesion region and classifies COVID-19 into 6 categories: healthy, ultraearly, early, rapid progression, consolidation, and dissipation stages.[120]

Different CT learning models have been developed to aid the diagnosis of COVID-19. The UNet++ takes the raw CT scan images as input and the segmented map as output, which is trained in Keras in an image-to-image manner. The sensitivity (true positive/positive), accuracy (true predictions/total number of cases), specificity (true negative/negative), positive prediction value (PPV), and negative prediction value (NPV) of the network were 100%, 92.59%, 81.82%, 88.89% and 100%, respectively. The average prediction time per patient is 41.34 s, and the reading time of the radiologist is reduced by 65%.[121] The 3D deep learning model with the classic ResNet-18 network can achieve CT image classification and segmentation with an accuracy rate of 86.7%.[122]

Deep pneumonia can assist the COVID-19 diagnosis in three steps. The first step is to extract the main regions of the lungs, and the second step is to design a Details Relation Extraction neural network (DRE-Net) to obtain image-level predictions. Finally, DRE-Net, which starts with a pretrained ResNet50 and an extra Feature Pyramid Network (FPN), is used to extract top-K details from each image and understand the importance of each detail through the attention module. The image level predictions can achieve 93% diagnostic sensitivity and can distinguish SARS-CoV-2 from bacterial-related pneumonia with 96% sensitivity. Moreover, their models were able to locate the main lesion features in 30 s, especially the ground-glass opacity.[123]

The transfer learning based on the modified Inception (M-Inception) consists of two parts: the first part uses a pretrained inception network to convert image data into one-dimensional feature vectors, and the second part uses a fully connected network for classification and prediction. The M-Inception reduces the dimension of the features before the classification layer and combines the Decision tree and AdaBoost as classifiers to improve the classification accuracy.[124] The Human-in-the-loop (HITL) strategy assists radiologists in performing automatic annotation and segmentation. The Dice similarity coefficient generated by the system between automatic and manual segmentation is 91.6% ± 10.0%. The Dice similarity coefficient is an index to measure the spatial overlap between the segmentation result and the ground truth. Fully manual delineation takes 1 to 5 h, but HITL reduces delineation time to 4 min after 3 iterative model updates.[125]

https://dx.doi.org/10.1021/acsinfecdis.0c00365
ACS Infect. Dis. 2020, 6, 1998−2016

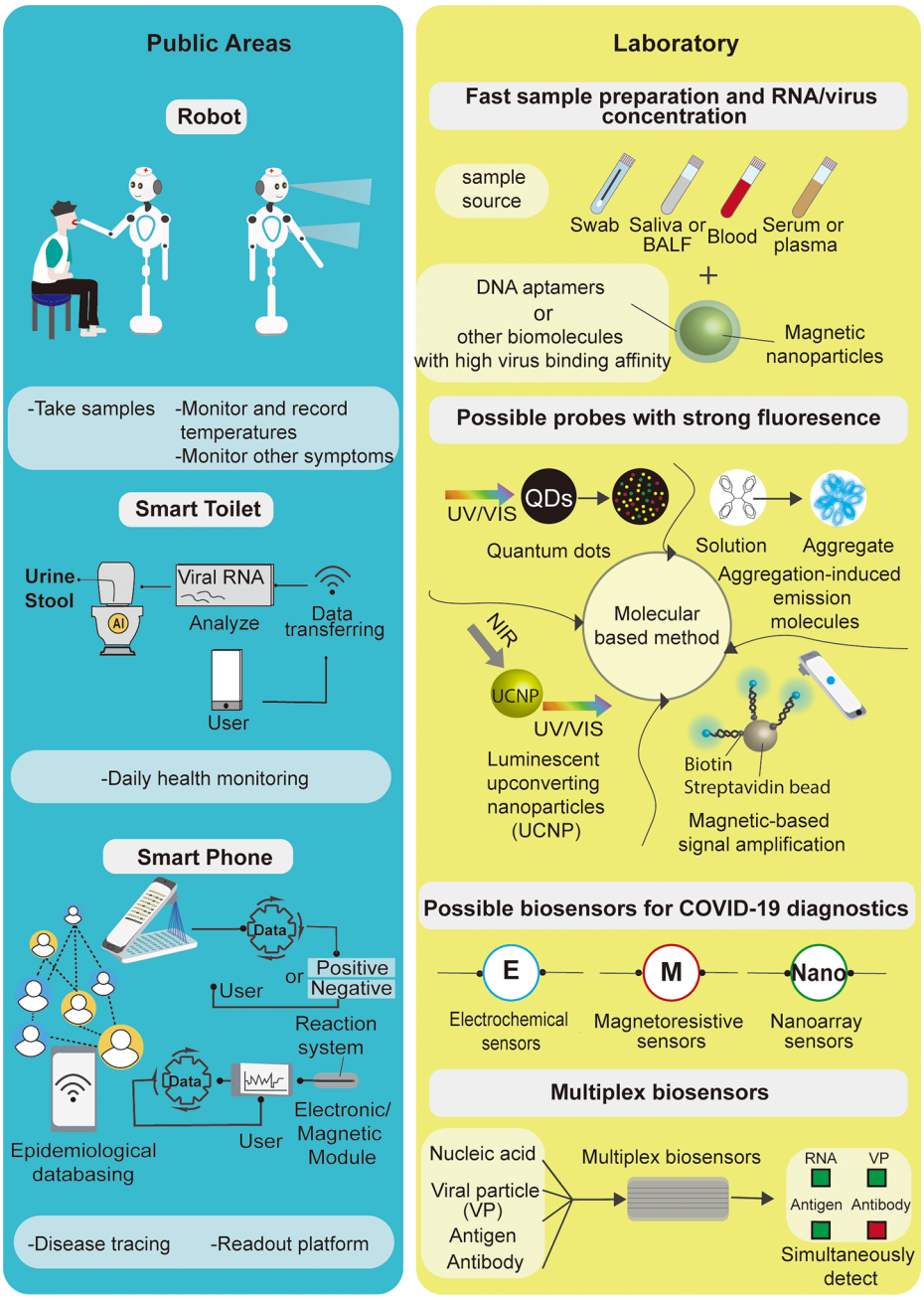

Figure 3. Possible strategies for the timely and efficiency diagnosis of COVID-19 in the future.

DeepLabv3 segmented CT images have a higher accuracy compared to U-net, SegNet, FCN, and DRUNET.[126]

However, the CT features of COVID-19 can easily be confused with other infections such as SARS-CoV-1 and seasonal flu. Integrating hierarchical CT features with other factors such as genetic, epidemiological, and clinical information for multimodal analysis will definitely further improve the efficiency and accuracy of COVID-19 diagnosis.[127]

■ PROSPECTS

Lessons learned from the past play a vital role to combat against the COVID-19 pandemic. In comparison with the SARS-CoV-1 outbreak in 2003, artificial intelligence (AI) has played a more important role, including contact tracing, evidence-based policymaking, and detection of COVID-19 infection in medical images (chest X-rays and CT scans). AI-enabled technologies, such as the AI robot, smart toilet, and smartphone, could provide valuable support for tracing, diagnostics, and therapeutics (Figure 3). The smart toilet, as a noninvasive device that can collect and analyze urine and stool, may become an important strategy for the diagnosis of COVID-19. Systems with cameras, pressure and motion sensors, and urinalysis strips have been used for health monitoring.[128] The robot can work in risky environments, thereby relieving the pressure on the frontline medical staff. The AI robot is capable of collecting throat swabs. The diagnostic and service robots will be deployed in crowded public places, such as customs, airports, ports, railway stations, etc. The mobile robot increases the efficiency and coverage of COVID-19 screening. Hopefully, with the consistent development of AI technologies, smarter and more powerful robotic

https://dx.doi.org/10.1021/acsinfecdis.0c00365
ACS Infect. Dis. 2020, 6, 1998−2016

systems under remote control with the ability to disinfect, deliver medications and food, measure temperature and vital signs, diagnose, and assist in transmission control will revolutionize weapons to fight against future viral epidemic outbreaks.

Asymptomatic and discharged COVID-19 patients are likely to transmit the virus to persons who are in close contact, making it challenging for the prevention and control of epidemics and requiring long-term monitoring and tracking. SARS-CoV-2 RNA has been detected in urine and stool samples of certain confirmed patients, even in asymptomatic cases,[129] indicating the high demand for ultrasensitive diagnostic techniques. A highly sensitive diagnostic platform can be developed by combining fluorescence resonance energy transfer, aggregation-induced emission molecules, and luminescent upconverting nanoparticles with unique optical properties (Figure 3). The magnetic properties of some nanoparticles, which enable the enrichment of fluorophores, offer the convenience of developing a smartphone-based readout system. The smartphone equipped with different optomechanical accessories, which enable the performance of brightfield, fluorescence, spectroscopy, or phase imaging, is a promising read-out platform. These devices make precise diagnostics possible in remote areas. The miniaturized sequencing devices make it available outside the laboratory for on-site applications. Synthetic biology has created novel molecular functions that can bring new capabilities to molecular diagnostics.[130] The development of DNA aptamers targeting viral proteins and conjugation with magnetic particles enable the enrichment of viruses during sampling and diagnostics.[131] The QDs with small volume and strong fluorescence are promising reporters for various fluorescence-based detection systems. The fluorescence polarization assay (FPA) takes advantage of molecular rotational properties to measure antigen−antibody or probe-target binding[132] with a small volume (2 μL) and a short diagnosis time (<20 min).[133] With a deeper understanding of viral−host interaction, novel dual biosensors, and the combination with isothermal amplification or immunoassay technology, the next-generation diagnostic techniques will be more robust, rapid, accurate, and easy to operate.

The SARS-CoV-2 genome undergoes rapid evolution during its transmission.[134−136] According to the available SARS-CoV-2 genome sequenced up to June 1, 2020, globally, 8309 single mutations have been observed in 15 140 SARS-CoV-2 isolates.[135] These mutations might affect the efficiency of oligonucleotide annealing and compromise the sensitivity and specificity of RT-PCR assays.[137,138] The target genes selected for molecular diagnosis should be relatively conserved. Meanwhile, multiple-target detection can minimize the risk of sensitivity loss due to unknown mutations. The kits of the early versions should be used with caution for the detection of prevalent SARS-CoV-2 subtypes. Genomic sequencing guides the design of nucleic acid-based diagnosis. The combination of multiple assays including viral RNA detection, lateral flow immunoassay, NGS, clinical symptoms, and CT imaging will provide a more accurate diagnosis. However, under real clinical conditions, there should be a balance between cost, time, accuracy, and specificity.

Vaccines and drugs for SARS-CoV-2 are the goals of global scientific competition. DNA vaccines are leading ahead of protein vaccines. The nanoparticle vaccine composed of a stabilized form of the respiratory syncytial virus (RSV) fusion (F) protein is fused to ferritin nanoparticle (Pre-F-NP) and modified with glycans to mask poorly neutralizing epitopes, thereby eliciting a potent immune response in mice and primates.[139] Sinovac Biotech has announced a vaccine that can protect monkeys from new coronavirus infections. Moreover, Moderna and CanSino have launched small vaccine clinical trials against COVID-19. Broad-spectrum antivirals inhibit SARS-CoV-2 in human airway epithelial cells and in mice.[140] Furthermore, a systematic study of viral−host interactions identifies 332 high-confidence SARS-CoV-2 human protein−protein interactions (PPI) and 66 druggable PPIs targeted by 69 compounds.[141] The receptor-binding domain is implicated in a viral attachment inhibitor and vaccine.[142] Besides, the structure of the main protease of SARS-CoV-2 has led to the development of two lead compounds with good pharmacokinetic properties in cell assays.[143] A new α-ketoamide inhibitor reveals a pronounced lung tropism and suitability for administration by inhalation.[144] CIRSPR is an alternative strategy for viral RNA inhibition and degradation.[145] The race to find COVID-19 treatments is accelerating and may take a few months or a few years or never succeed. The development of AI-assisted plug-and-read diagnostic robots and the enforcement of social contact patterns will be critical in preventing COVID-19 epidemics before the appearance of vaccines and drugs.[146]

■ AUTHOR INFORMATION

Corresponding Authors

Peiwu Qin − *Center of Precision Medicine and Healthcare, Tsinghua-Berkeley Shenzhen Institute, Shenzhen, Guangdong 518055, China;* orcid.org/0000-0002-7829-8973; Email: pwqin@sz.tsinghua.edu.cn

Ke Du − *Department of Mechanical Engineering, Rochester Institute of Technology, Rochester, New York 14623, United States;* orcid.org/0000-0002-6837-0927; Email: ke.du@rit.edu

Zhenhai Chu − *Southern University of Science and Technology Hospital, Shenzhen, Guangdong 518055, China;* Email: 412490573@qq.com

Authors

Xi Yuan − *Center of Precision Medicine and Healthcare, Tsinghua-Berkeley Shenzhen Institute, Shenzhen, Guangdong 518055, China*

Chengming Yang − *Southern University of Science and Technology Hospital, Shenzhen, Guangdong 518055, China*

Qian He − *Center of Precision Medicine and Healthcare, Tsinghua-Berkeley Shenzhen Institute, Shenzhen, Guangdong 518055, China*

Junhu Chen − *National Institute of Parasitic Diseases, Chinese Center for Disease Control and Prevention, Shanghai 200025, China*

Dongmei Yu − *Center of Precision Medicine and Healthcare, Tsinghua-Berkeley Shenzhen Institute, Shenzhen, Guangdong 518055, China; Department of Mechanics and Aerospace Engineering, Southern University of Science and Technology, Shenzhen, Guangdong 518055, China*

Jie Li − *Center of Precision Medicine and Healthcare, Tsinghua-Berkeley Shenzhen Institute, Shenzhen, Guangdong 518055, China; Kunming Dog Base of Police Security, Ministry of Public Security, Kunming, Yunnan 650204, China*

https://dx.doi.org/10.1021/acsinfecdis.0c00365
ACS Infect. Dis. 2020, 6, 1998−2016

Shiyao Zhai − *Center of Precision Medicine and Healthcare, Tsinghua-Berkeley Shenzhen Institute, Shenzhen, Guangdong 518055, China*

Zhifeng Qin − *Animal & Plant Inspection and Quarantine Technology Center, Shenzhen Customs District People's Republic of China, Shenzhen, Guangdong 518045, China*

Complete contact information is available at: https://pubs.acs.org/10.1021/acsinfecdis.0c00365

Author Contributions

†X.Y. and C.Y. contributed equally to this work. All authors were involved in the discussion and writing of the manuscript. All authors have read and agreed to the published version of the manuscript.

Notes

The authors declare no competing financial interest.

■ ACKNOWLEDGMENTS

This research is funded by Zhejiang University special scientific research fund for COVID-19 prevention and control and SUSTech Intelligent Health Engineering Platform (G02326403). The authors thank Wenrong He for the schematic design.

■ ABBREVIATIONS

COVID-19, coronavirus disease 2019; SARS-CoV-2, severe acute respiratory syndrome coronavirus 2; FNR, false-negative rate; SARS-CoV-1, severe acute respiratory syndrome coronavirus 1; CoVs, coronavirus; mNGS, metagenomic next-generation sequencing; ORFs, open reading frames; UTR, untranslated region; nts, nucleotide sequence; ACE2, angiotensin-converting enzyme 2; NPS, nasopharyngeal swab; OPS, oropharyngeal swab; BALF, bronchoalveolar lavage fluid; LoD, limit of detection; FET, field-effect transistor; QDs, quantum dots; HRP, horseradish peroxidase; PNA, peptide nucleic acid; qRT-PCR, quantitative reverse transcription-polymerase chain reaction; C_t, cycle threshold; NMPA, National Medical Products Administration; EUA, Emergency Use Authorization; FDA, Food and Drug Administration; CLIA, clinical laboratory improvement amendments; LAMP, loop-mediated isothermal amplification; RT-LAMP, reverse transcription LAMP; RPA, recombinase polymerase amplification; SSB, single-stranded DNA-binding protein; RCA, rolling circle amplification; fM, femtomolar; gRNAs, guide RNAs; pfu, plaque forming units; NPs, nanoparticles; GICA, gold immunochromatographic assay; MCLIA, magnetic chemiluminescence enzyme immunoassay; CT, computed tomography; DL, deep learning; PPV, positive prediction value; NPV, negative prediction value; HITL, Human-in-the-loop; AI, artificial intelligence; PPI, protein−protein interactions; Hel, helicase; ABI 7500, Applied Biosystems Real time PCR system 7500; GEC, genomic equivalents copies; TCID50, median tissue culture infectious dose per milliliter

■ REFERENCES

(1) World Health Organization. (accessed on 2020-08-01) *Coronavirus Disease (COVID-19) Outbreak Situation*, https://www.who.int/emergencies/diseases/novel-coronavirus-2019.

(2) Chen, Y., Liu, Q., and Guo, D. (2020) Emerging coronaviruses: Genome structure, replication, and pathogenesis. *J. Med. Virol. 92*, 418−423.

(3) Su, S., Wong, G., Shi, W., Liu, J., Lai, A. C. K., Zhou, J., Liu, W., Bi, Y., and Gao, G. F. (2016) Epidemiology, Genetic Recombination, and Pathogenesis of Coronaviruses. *Trends Microbiol. 24*, 490−502.

(4) Cui, J., Li, F., and Shi, Z.-L. (2019) Origin and Evolution of Pathogenic Coronaviruses. *Nat. Rev. Microbiol. 17*, 181−192.

(5) Wang, Y., Wang, Y., Chen, Y., and Qin, Q. (2020) Unique Epidemiological and Clinical Features of the Emerging 2019 Novel Coronavirus Pneumonia (COVID-19) Implicate Special Control Measures. *J. Med. Virol. 92*, 568−576.

(6) Chen, N., Zhou, M., Dong, X., Qu, J., Gong, F., Han, Y., Qiu, Y., Wang, J., Liu, Y., Wei, Y., Xia, J. a., Yu, T., Zhang, X., and Zhang, L. (2020) Epidemiological and Clinical Characteristics of 99 Cases of 2019 Novel Coronavirus Pneumonia in Wuhan, China: a Descriptive Study. *Lancet 395*, 507−513.

(7) Wang, C., Horby, P. W., Cao, B., Wu, P., Yang, s., Gao, H., Li, H., Tsang, T. K., Liao, Q., et al. (2014) Comparison of Patients Hospitalized with Influenza A Subtypes H7N9, H5N1, and 2009 Pandemic H1N1. *Clin. Infect. Dis. 58* (58), 1095−1103.

(8) Zhou, P., Yang, X.-L., Wang, X.-G., Hu, B., Zhang, L., Zhang, W., Si, H.-R., Zhu, Y., Li, B., Huang, C.-L., et al. (2020) A Pneumonia Outbreak Associated with a New Coronavirus of Probable Bat Origin. *Nature 579*, 270−273.

(9) Chen, L., Liu, W., Zhang, Q., Xu, K., Ye, G., Wu, W., Sun, Z., Liu, F., Wu, K., Zhong, B., Mei, Y., Zhang, W., Chen, Y., Li, Y., Shi, M., Lan, K., and Liu, Y. (2020) RNA Based Mngs Approach Identifies a Novel Human Coronavirus from Two Individual Pneumonia Cases in 2019 Wuhan Outbreak. *Emerging Microbes Infect. 9*, 313−319.

(10) Chan, J. F.-W., Kok, K.-H., Zhu, Z., Chu, H., To, K. K.-W., Yuan, S., and Yuen, K.-Y. (2020) Genomic Characterization Of the 2019 Novel Human-Pathogenic Coronavirus Isolated from a Patient with Atypical Pneumonia after Visiting Wuhan. *Emerging Microbes Infect. 9*, 221−236.

(11) Lu, R., Zhao, X., Li, J., Niu, P., Yang, B., Wu, H., Wang, W., Song, H., Huang, B., Zhu, N., et al. (2020) Genomic Characterisation and Epidemiology of 2019 Novel Coronavirus: Implications for Virus Origins and Receptor Binding. *Lancet 395*, 565−574.

(12) Paraskevis, D., Kostaki, E. G., Magiorkinis, G., Panayiotakopoulos, G., Sourvinos, G., and Tsiodras, S. (2020) Full-genome Evolutionary Analysis of the Novel Corona Virus (2019-nCoV) Rejects the Hypothesis of Emergence as a Result of a Recent Recombination Event. *Infect., Genet. Evol. 79*, 104212.

(13) Schoeman, D., and Fielding, B. C. (2019) Coronavirus envelope protein: current knowledge. *Virol. J. 16*, 69.

(14) Hoffmann, M., Kleine-Weber, H., Schroeder, S., Krüger, N., Herrler, T., Erichsen, S., Schiergens, T. S., Herrler, G., Wu, N. H., Nitsche, A., Müller, M. A., Drosten, C., and Pöhlmann, S. (2020) SARS-CoV-2 Cell Entry Depends on ACE2 and TMPRSS2 and Is Blocked by a Clinically Proven Protease Inhibitor. *Cell 181*, 271−280.

(15) de Wit, E., van Doremalen, N., Falzarano, D., and Munster, V. J. (2016) SARS and MERS: recent insights into emerging coronaviruses. *Nat. Rev. Microbiol. 14*, 523−34.

(16) Jiang, G., Ren, X., Liu, Y., Chen, H., Liu, W., Guo, Z., Zhang, Y., Chen, C., Zhou, J., Xiao, Q., and Shan, H. (2020) Application and Optimization of RT-PCR in Diagnosis of SARS-CoV-2 Infection. *medRxiv*, DOI: 10.1101/2020.02.25.20027755.

(17) Ai, T., Yang, Z., Hou, H., Zhan, C., Chen, C., Lv, W., Tao, Q., Sun, Z., and Xia, L. (2020) Correlation of Chest CT and RT-PCR Testing in Coronavirus Disease 2019 (COVID-19) in China: A report of 1014 cases. *Radiology 296*, E32.

(18) Matsuyama, S., Nao, N., Shirato, K., Kawase, M., Saito, S., Takayama, I., Nagata, N., Sekizuka, T., Katoh, H., Kato, F., Sakata, M., Tahara, M., Kutsuna, S., Ohmagari, N., Kuroda, M., Suzuki, T., Kageyama, T., and Takeda, M. (2020) Enhanced Isolation of SARS-CoV-2 by TMPRSS2-Expressing Cells. *Proc. Natl. Acad. Sci. U. S. A. 117*, 7001−7003.

(19) Wu, Y., Guo, G., Zheng, J., Xing, D., and Zhang, T. (2019) Fluorogenic "Photoclick" Labeling and Imaging of DNA with Coumarin-Fused Tetrazole in Vivo. *ACS. Sens. 4*, 44−51.

(20) Artika, I. M., and Ma'roef, C. N. (2017) Laboratory Biosafety For Handling Emerging Viruses. *Asian Pac. J. Trop. Biomed. 7*, 483−491.

(21) Yeh, Y. T., Gulino, K., Zhang, Y., Sabestien, A., Chou, T. W., Zhou, B., Lin, Z., Albert, I., Lu, H., Swaminathan, V., Ghedin, E., and Terrones, M. (2020) A Rapid and label-Free Platform for Virus Capture and Identification from Clinical Samples. *Proc. Natl. Acad. Sci. U. S. A. 117*, 895−901.

(22) Singh, R., Ma, D., Kimerling, L., Agarwal, A. M., and Anthony, B. W. (2019) Chemical Characterization of Aerosol Particles Using On-Chip Photonic Cavity Enhanced Spectroscopy. *ACS Sens. 4*, 571−577.

(23) Tancharoen, C., Sukjee, W., Thepparit, C., Jaimipuk, T., Auewarakul, P., Thitithanyanont, A., and Sangma, C. (2019) Electrochemical Biosensor Based on Surface Imprinting for Zika Virus Detection in Serum. *ACS Sens. 4*, 69−75.

(24) Tsutsui, M., Yokota, K., Yoshida, T., Hotehama, C., Kowada, H., Esaki, Y., Taniguchi, M., Washio, T., and Kawai, T. (2019) Identifying Single Particles in Air Using a 3D-Integrated Solid-State Pore. *ACS Sens. 4*, 748−755.

(25) Zhang, H., Xue, L., Huang, F., Wang, S., Wang, L., Liu, N., and Lin, J. (2019) A Capillary Biosensor for Rapid Detection of Salmonella Using Fe-nanocluster Amplification and Smart Phone Imaging. *Biosens. Bioelectron. 127*, 142−149.

(26) Im, H., Castro, C. M., Shao, H., Liong, M., Song, J., Pathania, D., Fexon, L., Min, C., Avila-Wallace, M., Zurkiya, O., Rho, J., Magaoay, B., Tambouret, R. H., Pivovarov, M., Weissleder, R., and Lee, H. (2015) Digital Diffraction Analysis Enables Low-Cost Molecular Diagnostics on A Smartphone. *Proc. Natl. Acad. Sci. U. S. A. 112*, 5613−8.

(27) Xia, Y., Chen, Y., Tang, Y., Cheng, G., Yu, X., He, H., Cao, G., Lu, H., Liu, Z., and Zheng, S. Y. (2019) Smartphone-Based Point-of-Care Microfluidic Platform Fabricated with a ZnO Nanorod Template for Colorimetric Virus Detection. *ACS Sens. 4*, 3298−3307.

(28) Sameiyan, E., Bagheri, E., Ramezani, M., Alibolandi, M., Abnous, K., and Taghdisi, S. M. (2019) DNA Origami-Based Aptasensors. *Biosens. Bioelectron. 143*, 111662.

(29) Liang, Y., Wu, C., Figueroa-Miranda, G., Offenhausser, A., and Mayer, D. (2019) Amplification of Aptamer Sensor Signals by Four Orders of Magnitude via Interdigitated Organic Electrochemical Transistors. *Biosens. Bioelectron. 144*, 111668.

(30) Hussein, H. A., Hassan, R. Y. A., El Nashar, R. M., Khalil, S. A., Salem, S. A., and El-Sherbiny, I. M. (2019) Designing and Fabrication of New VIP Biosensor for the Rapid And Selective Detection of Foot-And-Mouth Disease Virus (FMDV). *Biosens. Bioelectron. 141*, 111467.

(31) Sailapu, S. K., Macchia, E., Merino-Jimenez, I., Esquivel, J. P., Sarcina, L., Scamarcio, G., Minteer, S. D., Torsi, L., and Sabate, N. (2020) Standalone Operation of an EGOFET for Ultra-Sensitive Detection of HIV. *Biosens. Bioelectron. 156*, 112103.

(32) Zhu, H., Fohlerova, Z., Pekarek, J., Basova, E., and Neuzil, P. (2020) Recent Advances in Lab-on-a-Chip Technologies for Viral Diagnosis. *Biosens. Bioelectron. 153*, 112041.

(33) Yue, R., Li, Z., Wang, G., Li, J., and Ma, N. (2019) Logic Sensing of MicroRNA in Living Cells Using DNA-Programmed Nanoparticle Network with High Signal Gain. *ACS Sens. 4*, 250−256.

(34) Shi, L., Sun, Y., Mi, L., and Li, T. (2019) Target-Catalyzed Self-Growing Spherical Nucleic Acid Enzyme (SNAzyme) as a Double Amplifier for Ultrasensitive Chemiluminescence MicroRNA Detection. *ACS Sens. 4*, 3219−3226.

(35) Zopf, D., Pittner, A., Dathe, A., Grosse, N., Csaki, A., Arstila, K., Toppari, J. J., Schott, W., Dontsov, D., Uhlrich, G., Fritzsche, W., and Stranik, O. (2019) Plasmonic Nanosensor Array for Multiplexed DNA-based Pathogen Detection. *ACS Sens. 4*, 335−343.

(36) Feng, X., Han, T., Xiong, Y., Wang, S., Dai, T., Chen, J., Zhang, X., and Wang, G. (2019) Plasmon-Enhanced Electrochemiluminescence of Silver Nanoclusters for microRNA Detection. *ACS Sens. 4*, 1633−1640.

(37) Lee, T., Mohammadniaei, M., Zhang, H., Yoon, J., Choi, H. K., Guo, S., Guo, P., and Choi, J. W. (2020) Single Functionalized pRNA/Gold Nanoparticle for Ultrasensitive MicroRNA Detection Using Electrochemical Surface-Enhanced Raman Spectroscopy. *Adv. Sci. 7*, 1902477.

(38) Wang, M., Yin, H., Zhou, Y., Sui, C., Wang, Y., Meng, X., Waterhouse, G. I. N., and Ai, S. (2019) Photoelectrochemical Biosensor for Microrna Detection Based on a MoS_2/g-C_3N_4/black TiO_2 Heterojunction with Histostar@AuNPs for Signal Amplification. *Biosens. Bioelectron. 128*, 137−143.

(39) Guo, W. J., Wu, Z., Yang, X. Y., Pang, D. W., and Zhang, Z. L. (2019) Ultrasensitive Electrochemical Detection of Microrna-21 with Wide Linear Dynamic Range Based on Dual Signal Amplification. *Biosens. Bioelectron. 131*, 267−273.

(40) Eaton, S. L., Proudfoot, C., Lillico, S. G., Skehel, P., Kline, R. A., Hamer, K., Rzechorzek, N. M., Clutton, E., Gregson, R., King, T., O'Neill, C. A., Cooper, J. D., Thompson, G., Whitelaw, C. B., and Wishart, T. M. (2019) CRISPR/Cas9Mediated Generation of an Ovine Model for Infantile Neuronal Ceroid Lipofuscinosis (CLN1 disease). *Sci. Rep. 9*, 9891.

(41) Fortunati, S., Rozzi, A., Curti, F., Giannetto, M., Corradini, R., and Careri, M. (2019) Novel Amperometric Genosensor Based on Peptide Nucleic Acid (PNA) Probes Immobilized on Carbon Nanotubes-Screen Printed Electrodes for the Determination of Trace Levels of Non-Amplified DNA in Genetically Modified (GM) Soy. *Biosens. Bioelectron. 129*, 7−14.

(42) Campos, R., Borme, J., Guerreiro, J. R., Machado, G., Jr., Cerqueira, M. F., Petrovykh, D. Y., and Alpuim, P. (2019) Attomolar Label-Free Detection of DNA Hybridization with Electrolyte-Gated Graphene Field-Effect Transistors. *ACS Sens. 4*, 286−293.

(43) Kaur, A., Sapkota, K., and Dhakal, S. (2019) Multiplexed Nucleic Acid Sensing with Single-Molecule FRET. *ACS Sens. 4*, 623−633.

(44) Ribes, A., Aznar, E., Santiago-Felipe, S., Xifre-Perez, E., Tormo-Mas, M. A., Peman, J., Marsal, L. F., and Martinez-Manez, R. (2019) Selective and Sensitive Probe Based in Oligonucleotide-Capped Nanoporous Alumina for the Rapid Screening of Infection Produced by Candida albicans. *ACS Sens. 4*, 1291−1298.

(45) Wang, J. W., Karnaushenko, D., Medina-Sanchez, M., Yin, Y., Ma, L. B., and Schmidt, O. G. (2019) Three-Dimensional Microtubular Devices for Lab-on-a-Chip Sensing Applications. *Acs Sens. 4*, 1476−1496.

(46) Chen, X., Miller, A., Cao, S., Gan, Y., Zhang, J., He, Q., Wang, R. Q., Yong, X., Qin, P., Lapizco-Encinas, B. H., and Du, K. (2020) Rapid Escherichia coli Trapping and Retrieval from Bodily Fluids via a Three-Dimensional Bead-Stacked Nanodevice. *ACS Appl. Mater. Interfaces 12*, 7888−7896.

(47) Hass, K. N., Bao, M., He, Q., Park, M., Qin, P., and Du, K. (2020) Integrated Micropillar Polydimethylsiloxane Accurate CRISPR Detection (IMPACT) System for Rapid Viral DNA Sensing. *bioRxiv*, DOI: 10.1101/2020.03.17.994137.

(48) Oh, S., Lee, M. K., and Chi, S. W. (2019) Single-Molecule-Based Detection of Conserved Influenza A Virus RNA Promoter Using a Protein Nanopore. *ACS Sens. 4*, 2849−2853.

(49) Canady, T. D., Li, N., Smith, L. D., Lu, Y., Kohli, M., Smith, A. M., and Cunningham, B. T. (2019) Digital-Resolution Detection of MicroRNA with Single-Base Selectivity by Photonic Resonator Absorption Microscopy. *Proc. Natl. Acad. Sci. U. S. A. 116*, 19362−19367.

(50) Wang, L., Zhang, H., Wang, C., Xu, Y., Su, J., Wang, X., Liu, X., Feng, D., Wang, L., Zuo, X., Shi, J., Ge, Z., Fan, C., and Mi, X. (2019) Poly-Adenine-Mediated Spherical Nucleic Acids for Strand Displacement-Based DNA/RNA Detection. *Biosens. Bioelectron. 127*, 85−91.

(51) Li, M., Chen, T., Gooding, J. J., and Liu, J. (2019) Review of Carbon and Graphene Quantum Dots for Sensing. *ACS Sens. 4*, 1732−1748.

(52) Gao, M., Wu, R., Mei, Q., Zhang, C., Ling, X., Deng, S., He, H., and Zhang, Y. (2019) Upconversional Nanoprobes with Highly Efficient Energy Transfer for Ultrasensitive Detection of Alkaline Phosphatase. *ACS Sens. 4*, 2864−2868.

(53) Harvey, J. D., Baker, H. A., Ortiz, M. V., Kentsis, A., and Heller, D. A. (2019) HIV Detection via a Carbon Nanotube RNA Sensor. *ACS Sens. 4*, 1236−1244.
(54) Kupferschmidt, K. (2020) Genome Analyses Help Track Coronavirus' Moves. *Science 367*, 1176−1177.
(55) Wang, Y., Cao, T., Ko, J., Shen, Y., Zong, W., Sheng, K., Cao, W., Sun, S., Cai, L., Zhou, Y. L., Zhang, X. X., Zong, C., Weissleder, R., and Weitz, D. (2020) Dissolvable Polyacrylamide Beads for High-Throughput Droplet DNA Barcoding. *Adv. Sci. 7*, 1903463.
(56) Jin, Y.-H., Cai, L., Cheng, Z.-S., Cheng, H., Deng, T., Fan, Y.-P., Fang, C., Huang, D., Huang, L.-Q., Huang, Q., et al. (2020) A Rapid Advice Guideline for the Diagnosis and Treatment of 2019 Novel Coronavirus (2019-nCoV) Infected Pneumonia (standard version). *Mil. Med. Res. 7*, 4.
(57) National Medical Products Administration. (accessed on 2020-05-11) *New novel coronavirus detection products approved by the National Medical Products Administration*, http://www.nmpa.gov.cn/WS04/CL2056/375802.html.
(58) United States Food and Drug Administration. (accessed on 2020-05-11) *Emergency Use Authorizations*, https://www.fda.gov/medical-devices/emergency-situations-medical-devices/emergency-use-authorizations#covid19ivd.
(59) Wang, Y., Kang, H., Liu, X., and Tong, Z. (2020) Combination of RT-qPCR Testing and Clinical Features for Diagnosis of COVID-19 Facilitates Management of SARS-CoV-2 Outbreak. *J. Med. Virol. 92*, 538−539.
(60) Shi, H., Han, X., Jiang, N., Cao, Y., Alwalid, O., Gu, J., Fan, Y., and Zheng, C. (2020) Radiological Findings from 81 Patients with COVID-19 Pneumonia in Wuhan, China: a Descriptive Study. *Lancet Infect. Dis. 20*, 425−434.
(61) Wang, C., Liu, Z., Chen, Z., Huang, X., Xu, M., He, T., and Zhang, Z. (2020) The Establishment of Reference Sequence for SARS-CoV-2 and Variation Analysis. *J. Med. Virol. 92*, 667−674.
(62) Zhou, S., Gou, T., Hu, J., Wu, W., Ding, X., Fang, W., Hu, Z., and Mu, Y. (2019) A Highly Integrated Real-Time Digital PCR Device for Accurate DNA Quantitative Analysis. *Biosens. Bioelectron. 128*, 151−158.
(63) Yu, L., Wu, S., Hao, X., Li, X., Liu, X., Ye, S., Han, H., Dong, X., Li, X., Li, J., et al. (2020) Rapid Colorimetric Detection of COVID-19 Coronavirus Using a Reverse Transcriptional Loop-Mediated Isothermal Amplification (RT-LAMP) Diagnostic Platform: iLACO. *Clin. Chem. 66*, 975−977.
(64) Soares, R. R. G., Neumann, F., Caneira, C. R. F., Madaboosi, N., Ciftci, S., Hernandez-Neuta, I., Pinto, I. F., Santos, D. R., Chu, V., Russom, A., Conde, J. P., and Nilsson, M. (2019) Silica Bead-Based Microfluidic Device with Integrated Photodiodes for the Rapid Capture and Detection of Rolling Circle Amplification Products in the Femtomolar Range. *Biosens. Bioelectron. 128*, 68−75.
(65) Beamish, E., Tabard-Cossa, V., and Godin, M. (2019) Programmable DNA Nanoswitch Sensing with Solid-State Nanopores. *ACS Sens. 4*, 2458−2464.
(66) Faria, H. A. M., and Zucolotto, V. (2019) Label-Free Electrochemical DNA Biosensor for Zika Virus Identification. *Biosens. Bioelectron. 131*, 149−155.
(67) Nie, Y., Zhang, X., Zhang, Q., Liang, Z., Ma, Q., and Su, X. (2020) A Novel High Efficient Electrochemiluminescence Sensor Based on Reductive Cu(I) Particles Catalyzed Zn-doped MoS2 QDs for HPV 16 DNA Determination. *Biosens. Bioelectron. 160*, 112217.
(68) Zhao, H., Ye, D., Mao, X., Li, F., Xu, J., Li, M., and Zuo, X. (2019) Stepping Gating of Ion Channels on Nanoelectrode via DNA Hybridization for Label-Free DNA Detection. *Biosens. Bioelectron. 133*, 141−146.
(69) Divya, K. P., Karthikeyan, R., Sinduja, B., Anancia Grace, A., John, S. A., Hahn, J. H., and Dharuman, V. (2019) Carbon Dots Stabilized Silver-Lipid Nano Hybrids for Sensitive Label Free DNA Detection. *Biosens. Bioelectron. 133*, 48−54.
(70) Sun, Y., Peng, Z., Li, H., Wang, Z., Mu, Y., Zhang, G., Chen, S., Liu, S., Wang, G., Liu, C., Sun, L., Man, B., and Yang, C. (2019) Suspended CNT-Based FET Sensor for Ultrasensitive and Label-Free Detection of DNA Hybridization. *Biosens. Bioelectron. 137*, 255−262.
(71) Lin, X., Huang, X., Urmann, K., Xie, X., and Hoffmann, M. R. (2019) Digital Loop-Mediated Isothermal Amplification on a Commercial Membrane. *ACS Sens. 4*, 242−249.
(72) Chen, B. J., Mani, V., Huang, S. T., Hu, Y. C., and Shan, H. P. (2019) Bisintercalating DNA Redox Reporters for Real-Time Electrochemical qLAMP. *Biosens. Bioelectron. 129*, 277−283.
(73) Munoz, H. E., Riche, C. T., Kong, J. E., van Zee, M., Garner, O. B., Ozcan, A., and Di Carlo, D. (2020) Fractal LAMP: Label-Free Analysis of Fractal Precipitate for Digital Loop-Mediated Isothermal Nucleic Acid Amplification. *ACS Sens. 5*, 385−394.
(74) Schmid-Burgk, J. L., Li, D., Feldman, D., Słabicki, M., Borrajo, J., Strecker, J., Cleary, B., Regev, A., and Zhang, F. (2020) LAMP-Seq: Population-Scale COVID-19 Diagnostics Using a Compressed Barcode Space. *bioRxiv*, DOI: 10.1101/2020.04.06.025635.
(75) Kampeera, J., Pasakon, P., Karuwan, C., Arunrut, N., Sappat, A., Sirithammajak, S., Dechokiattawan, N., Sumranwanich, T., Chaivisuthangkura, P., Ounjai, P., Chankhamhaengdecha, S., Wisitsoraat, A., Tuantranont, A., and Kiatpathomchai, W. (2019) Point-of-care rapid detection of Vibrio parahaemolyticus in seafood using loop-mediated isothermal amplification and graphene-based screen-printed electrochemical sensor. *Biosens. Bioelectron. 132*, 271−278.
(76) Azizi, M., Zaferani, M., Cheong, S. H., and Abbaspourrad, A. (2019) Pathogenic Bacteria Detection Using RNA-Based Loop-Mediated Isothermal-Amplification-Assisted Nucleic Acid Amplification via Droplet Microfluidics. *ACS Sens. 4*, 841−848.
(77) Yee, E. H., and Sikes, H. D. (2020) Polymerization-Based Amplification for Target-Specific Colorimetric Detection of Amplified Mycobacterium tuberculosis DNA on Cellulose. *ACS Sens. 5*, 308−312.
(78) Piepenburg, O., Williams, C. H., Stemple, D. L., and Armes, N. A. (2006) DNA Detection Using Recombination Proteins. *PLoS Biol. 4*, e204.
(79) El-Tholoth, M., Bau, H. H., and Song, J. (2020) A Single and Two-Stage, Closed-Tube, Molecular Test for the 2019 Novel Coronavirus (COVID-19) at Home, Clinic, and Points of Entry. *ChemRxiv*, DOI: 10.26434/chemrxiv.11860137.
(80) Tian, W., Li, P., He, W., Liu, C., and Li, Z. (2019) Rolling Circle Extension-Actuated Loop-Mediated Isothermal Amplification (RCA-LAMP) for Ultrasensitive Detection of MicroRNAs. *Biosens. Bioelectron. 128*, 17−22.
(81) Tian, B., Fock, J., Minero, G. A. S., and Hansen, M. F. (2020) Nicking-Assisted on-Loop and off-Loop Enzymatic Cascade Amplification for Optomagnetic Detection of a Highly Conserved Dengue Virus Sequence. *Biosens. Bioelectron. 160*, 112219.
(82) Ye, X., Li, L., Li, J., Wu, X., Fang, X., and Kong, J. (2019) Microfluidic-CFPA Chip for the Point-of-Care Detection of African Swine Fever Virus with a Median Time to Threshold in about 10 min. *ACS Sens. 4*, 3066−3071.
(83) Zhang, F., Abudayyeh, O. O., and Jonathan, S. G. (accessed on 2020-05-01) *A protocol for detection of COVID-19 using CRISPR diagnostics*, https://www.broadinstitute.org/files/publications/special/COVID-19%20detection%20(updated).pdf.
(84) Broughton, J. P., Deng, X., Yu, G., Fasching, C. L., Servellita, V., Singh, J., Miao, X., Streithorst, J. A., Granados, A., Sotomayor-Gonzalez, A., Zorn, K., Gopez, A., Hsu, E., Gu, W., Miller, S., Pan, C. Y., Guevara, H., Wadford, D. A., Chen, J. S., and Chiu, C. Y. (2020) CRISPR-Cas12-Based Detection of SARS-CoV-2. *Nat. Biotechnol. 38*, 870−874.
(85) Li, Z., Yi, Y., Luo, X., Xiong, N., Liu, Y., Li, S., Sun, R., Wang, Y., Hu, B., Chen, W., et al. (2020) Development and Clinical Application of A Rapid IgM-IgG Combined Antibody Test for SARS-CoV-2 Infection Diagnosis. *J. Med. Virol.*, 1−7.
(86) Anzalone, A. V., Randolph, P. B., Davis, J. R., Sousa, A. A., Koblan, L. W., Levy, J. M., Chen, P. J., Wilson, C., Newby, G. A., Raguram, A., et al. (2019) Search-and-Replace Genome Editing

Without Double-Strand Breaks or Donor DNA. *Nature 576*, 149−157.
(87) Qin, P., Parlak, M., Kuscu, C., Bandaria, J., Mir, M., Szlachta, K., Singh, R., Darzacq, X., Yildiz, A., and Adli, M. (2017) Live Cell Imaging of Low- and Non-Repetitive Chromosome Loci Using CRISPR-Cas9. *Nat. Commun. 8*, 14725.
(88) Flint, M., Chatterjee, P., Lin, D. L., McMullan, L. K., Shrivastava-Ranjan, P., Bergeron, É., Lo, M. K., Welch, S. R., Nichol, S. T., Tai, A. W., et al. (2019) A Genome-Wide CRISPR Screen Identifies N-Acetylglucosamine-1-Phosphate Transferase as a Potential Antiviral Target for Ebola Virus. *Nat. Commun. 10*, 1−13.
(89) He, Q., Yu, D., Bao, M., Korensky, G., Chen, J., Shin, M., Kim, J., Park, M., Qin, P., and Du, K. (2020) High-throughput and All-Solution Phase African Swine Fever Virus (ASFV) Detection Using CRISPR-Cas12a and Fluorescence Based Point-of-Care System. *Biosens. Bioelectron. 154*, 112068.
(90) Qin, P., Park, M., Alfson, K. J., Tamhankar, M., Carrion, R., Patterson, J. L., Griffiths, A., He, Q., Yildiz, A., Mathies, R., et al. (2019) Rapid and Fully Microfluidic Ebola Virus Detection with CRISPR-Cas13a. *ACS sens. 4*, 1048−1054.
(91) Kellner, M. J., Koob, J. G., Gootenberg, J. S., Abudayyeh, O. O., and Zhang, F. (2019) SHERLOCK: Nucleic Acid Detection with CRISPR Nucleases. *Nat. Protoc. 14*, 2986−3012.
(92) Hou, T., Zeng, W., Yang, M., Chen, W., Ren, L., Ai, J., Wu, J., Liao, Y., Gou, X., Li, Y., Wang, X., Su, H., Gu, B., Wang, J., and Xu, T. (2020) Development and Evaluation of A CRISPR-based Diagnostic For 2019-novel Coronavirus. *medRxiv*, DOI: 10.1101/2020.02.22.20025460.
(93) Weckman, N. E., Ermann, N., Gutierrez, R., Chen, K., Graham, J., Tivony, R., Heron, A., and Keyser, U. F. (2019) Multiplexed DNA Identification Using Site Specific dCas9 Barcodes and Nanopore Sensing. *ACS Sens. 4*, 2065−2072.
(94) Reddington, K., Tuite, N., Barry, T., O'Grady, J., and Zumla, A. (2013) Advances in multiparametric molecular diagnostics technologies for respiratory tract infections. *Curr. Opin. Pulm. Med. 19*, 298−304.
(95) Dey, P., Fabri-Faja, N., Calvo-Lozano, O., Terborg, R. A., Belushkin, A., Yesilkoy, F., Fabrega, A., Ruiz-Rodriguez, J. C., Ferrer, R., Gonzalez-Lopez, J. J., Estevez, M. C., Altug, H., Pruneri, V., and Lechuga, L. M. (2019) Label-free Bacteria Quantification in Blood Plasma by a Bioprinted Microarray Based Interferometric Point-of-Care Device. *ACS Sens 4*, 52−60.
(96) Hernandez-Neuta, I., Neumann, F., Brightmeyer, J., Ba Tis, T., Madaboosi, N., Wei, Q., Ozcan, A., and Nilsson, M. (2019) Smartphone-Based Clinical Diagnostics: Towards Democratization of Evidence-Based Health Care. *J. Intern. Med. 285*, 19−39.
(97) Zhu, H., Hu, S. H., Jona, G., Zhu, X. W., Kreiswirth, N., Willey, B. M., Mazzulli, T., Liu, G. Z., Song, Q. F., Chen, P., Cameron, M., Tyler, A., Wang, J., Wen, J., Chen, W. J., Compton, S., and Snyder, M. (2006) Severe Acute Respiratory Syndrome Diagnostics Using a Coronavirus Protein Microarray. *Proc. Natl. Acad. Sci. U. S. A. 103*, 4011−4016.
(98) Yershov, G., Barsky, V., Belgovskiy, A., Kirillov, E., Kreindlin, E., Ivanov, I., Parinov, S., Guschin, D., Drobishev, A., Dubiley, S., and Mirzabekov, A. (1996) DNA Analysis and Diagnostics on Oligonucleotide Microchips. *Proc. Natl. Acad. Sci. U. S. A. 93*, 4913−8.
(99) Jiang, S., Du, L., and Shi, Z. (2020) An Emerging Coronavirus Causing Pneumonia Outbreak in Wuhan, China: Calling for Developing Therapeutic and Prophylactic Strategies. *Emerging Microbes Infect. 9*, 275−277.
(100) Wee, S., Alli-Shaik, A., Kek, R., Swa, H. L. F., Tien, W. P., Lim, V. W., Leo, Y. S., Ng, L. C., Hapuarachchi, H. C., and Gunaratne, J. (2019) Multiplex Targeted Mass Spectrometry Assay for One-Shot Flavivirus Diagnosis. *Proc. Natl. Acad. Sci. U. S. A. 116*, 6754−6759.
(101) Dai, L., Li, Y., Wang, Y., Luo, X., Wei, D., Feng, R., Yan, T., Ren, X., Du, B., and Wei, Q. (2019) A Prostate-Specific Antigen Electrochemical Immunosensor Based on Pd NPs Functionalized Electroactive Co-MOF Signal Amplification Strategy. *Biosens. Bioelectron. 132*, 97−104.
(102) Mayall, R. M., Renaud-Young, M., Gawron, E., Luong, S., Creager, S., and Birss, V. I. (2019) Enhanced Signal Amplification in a Toll-like Receptor-4 Biosensor Utilizing Ferrocene-Terminated Mixed Monolayers. *ACS Sens. 4*, 143−151.
(103) Pandit, S., Banerjee, T., Srivastava, I., Nie, S., and Pan, D. (2019) Machine Learning-Assisted Array-Based Biomolecular Sensing Using Surface-Functionalized Carbon Dots. *ACS Sens. 4*, 2730−2737.
(104) Xia, C., Zhu, S., Feng, T., Yang, M., and Yang, B. (2019) Evolution and Synthesis of Carbon Dots: From Carbon Dots to Carbonized Polymer Dots. *Adv. Sci. 6*, 1901316.
(105) Li, W. S., Fan, G. C., Gao, F. X., Cui, Y. G., Wang, W., and Luo, X. L. (2019) High-activity Fe_3O_4 Nanozyme as Signal Amplifier: A simple, Low-Cost but Efficient Strategy for Ultrasensitive Photoelectrochemical Immunoassay. *Biosens. Bioelectron. 127*, 64−71.
(106) Li, D., Jiang, L., Piper, J. A., Maksymov, I. S., Greentree, A. D., Wang, E., and Wang, Y. (2019) Sensitive and Multiplexed SERS Nanotags for the Detection of Cytokines Secreted by Lymphoma. *ACS Sens. 4*, 2507−2514.
(107) Lee, S., Ahn, S., Chakkarapani, S. K., and Kang, S. H. (2019) Supersensitive Detection of the Norovirus Immunoplasmon by 3D Total Internal Reflection Scattering Defocus Microscopy with Wavelength-Dependent Transmission Grating. *ACS Sens. 4*, 2515−2523.
(108) Coudron, L., McDonnell, M. B., Munro, I., McCluskey, D. K., Johnston, I. D., Tan, C. K. L., and Tracey, M. C. (2019) Fully integrated digital microfluidics platform for automated immunoassay; A versatile tool for rapid, specific detection of a wide range of pathogens. *Biosens. Bioelectron. 128*, 52−60.
(109) Herr, A. E., Hatch, A. V., Throckmorton, D. J., Tran, H. M., Brennan, J. S., Giannobile, W. V., and Singh, A. K. (2007) Microfluidic Immunoassays as Rapid Saliva-Based Clinical Diagnostics. *Proc. Natl. Acad. Sci. U. S. A. 104*, 5268−5273.
(110) Zhang, J., Liu, J., Li, N., Liu, Y., Ye, R., Qin, X., and Zheng, R. (2020) Serological Detection of 2019-nCoV Respond to the Epidemic: A Useful Complement to Nucleic Acid Testing. *medRxiv*, DOI: 10.1101/2020.03.04.20030916.
(111) Cai, X., Chen, J., Hu, J., Long, Q., Deng, H., Fan, K., Liao, P., Liu, B., Wu, G., and Chen, Y. (2020) A Peptide-based Magnetic Chemiluminescence Enzyme Immunoassay for Serological Diagnosis of Corona Virus Disease 2019 (COVID-19). *J. Infect. Dis. 222*, 189−193.
(112) Xiang, J., Yan, M., Li, H., Liu, T., Lin, C., Huang, S., and Shen, C. (2020) Evaluation of Enzyme-Linked Immunoassay and Colloidal Gold-Immunochromatographic Assay Kit for Detection of Novel Coronavirus (SARS-Cov-2) Causing an Outbreak of Pneumonia (COVID-19). *medRxiv*, DOI: 10.1101/2020.02.27.20028787.
(113) Natesan, M., Wu, S. W., Chen, C. I., Jensen, S. M. R., Karlovac, N., Dyas, B. K., Mudanyali, O., and Ulrich, R. G. (2019) A Smartphone-Based Rapid Telemonitoring System for Ebola and Marburg Disease Surveillance. *ACS Sens 4*, 61−68.
(114) Nandhakumar, P., Ichzan, A. M., Lee, N. S., Yoon, Y. H., Ma, S., Kim, S., and Yang, H. (2019) Carboxyl Esterase-Like Activity of DT-Diaphorase and Its Use for Signal Amplification. *ACS Sens. 4*, 2966−2973.
(115) Tate, J., and Ward, G. (2004) Interferences in Immunoassay. *Clin. Biochem. Rev. 25*, 105−120.
(116) Guntner, A. T., Abegg, S., Konigstein, K., Gerber, P. A., Schmidt-Trucksass, A., and Pratsinis, S. E. (2019) Breath Sensors for Health Monitoring. *ACS. Sens. 4*, 268−280.
(117) Chen, A., Halton, A. J., Rhoades, R. D., Booth, J. C., Shi, X., Bu, X., Wu, N., and Chae, J. (2019) Wireless Wearable Ultrasound Sensor on a Paper Substrate to Characterize Respiratory Behavior. *ACS Sens. 4*, 944−952.
(118) Chung, M., Bernheim, A., Mei, X., Zhang, N., Huang, M., Zeng, X., Cui, J., Xu, W., Yang, Y., Fayad, Z. A., Jacobi, A., Li, K., Li, S., and Shan, H. (2020) CT Imaging Features of 2019 Novel Coronavirus (2019-nCoV). *Radiology 295*, 202−207.

(119) Xiong, Y., Sun, D., Liu, Y., Fan, Y., Zhao, L., Li, X., and Zhu, W. (2020) Clinical and High-Resolution CT Features of the COVID-19 Infection: Comparison of the Initial and Follow-up Changes. *Invest. Radiol. 55*, 332−339.

(120) Liu, Y., Liu, G., and Zhang, Q. (2019) Deep Learning and Medical Diagnosis. *Lancet 394*, 1709−1710.

(121) Chen, J., Wu, L., Zhang, J., Zhang, L., Gong, D., Zhao, Y., Hu, S., Wang, Y., Hu, X., and Zheng, B. (2020) Deep Learning-Based Model for Detecting 2019 Novel Coronavirus Pneumonia on High-Resolution Computed Tomography: a Prospective Study. *medRxiv*, DOI: 10.1101/2020.02.25.20021568.

(122) Xu, X., Jiang, X., Ma, C., Du, P., Li, X., Lv, S., Yu, L., Chen, Y., Su, J., Lang, G., et al. (2020) A Deep Learning System to Screen Novel Coronavirus Disease 2019 Pneumonia. *Engineering*, DOI: 10.1016/j.eng.2020.04.010.

(123) Song, Y., Zheng, S., Li, L., Zhang, X., Zhang, X., Huang, Z., Chen, J., Zhao, H., Jie, Y., and Wang, R. (2020) Deep learning Enables Accurate Diagnosis of Novel Coronavirus (COVID-19) with CT images. *medRxiv*, DOI: 10.1101/2020.02.23.20026930.

(124) Wang, S., Kang, B., Ma, J., Zeng, X., Xiao, M., Guo, J., Cai, M., Yang, J., Li, Y., and Meng, X. (2020) A Deep Learning Algorithm Using CT Images to Screen for Corona Virus Disease (COVID-19). *medRxiv*, DOI: 10.1101/2020.02.14.20023028.

(125) Shan, F., Gao, Y., Wang, J., Shi, W., Shi, N., Han, M., Xue, Z., Shen, D., and Shi, Y. (2020) Lung Infection Quantification of COVID-19 in CT Images with Deep Learning. *arXiv*, https://arxiv.org/abs/2003.04655.

(126) Zhang, K., Liu, X., Shen, J., Li, Z., Sang, Y., Wu, X., Cha, Y., Liang, W., Wang, C., Wang, K., Ye, L., Gao, M., Zhou, Z., Li, L., Wang, J., Yang, Z., Cai, H., Xu, J., Yang, L., Cai, W., Xu, W., Wu, S., Zhang, W., Jiang, S., Zheng, L., Zhang, X., Wang, L., Lu, L., Li, J., Wu, H., Wang, W., Li, O., Zhang, C., Liang, L., Wu, T., Deng, R., Wei, K., Zhou, Y., Chen, T., Yiu-Nam Lau, J., Fok, M., He, J., Lin, T., Li, W., and Wang, G. (2020) Clinically Applicable AI System for Accurate Diagnosis, Quantitative Measurements and Prognosis of COVID-19 Pneumonia Using Computed Tomography. *Cell 181*, 1423−1433.e11.

(127) Han, W., Quan, B., Guo, Y., Zhang, J., Lu, Y., Feng, G., Wu, Q., Fang, F., Cheng, L., Jiao, N., Li, X., and Chen, Q. (2020) The Course of Clinical Diagnosis and Treatment of a Case Infected with Coronavirus Disease 2019. *J. Med. Virol. 92*, 461−463.

(128) Park, S.-m., Won, D. D., Lee, B. J., Escobedo, D., Esteva, A., Aalipour, A., Ge, T. J., Kim, J. H., Suh, S., Choi, E. H., Lozano, A. X., Yao, C., Bodapati, S., Achterberg, F. B., Kim, J., Park, H., Choi, Y., Kim, W. J., Yu, J. H., Bhatt, A. M., Lee, J. K., Spitler, R., Wang, S. X., and Gambhir, S. S. (2020) A mountable toilet system for personalized health monitoring via the analysis of excreta. *Nat. Biomed. Eng. 4*, 624−635.

(129) Jiang, X., Luo, M., Zou, Z., Wang, X., Chen, C., and Qiu, J. (2020) Asymptomatic SARS-CoV-2 Iinfected Case with Viral Detection Positive in Stool but Negative in Nasopharyngeal Samples Lasts for 42 days. *J. Med. Virol.*, DOI: 10.1002/jmv.25941.

(130) Slomovic, S., Pardee, K., and Collins, J. J. (2015) Synthetic Biology Devices for in Vitro and in Vivo Diagnostics. *Proc. Natl. Acad. Sci. U. S. A. 112*, 14429−35.

(131) Zhang, K., Yue, Y., Wu, S., Liu, W., Shi, J., and Zhang, Z. (2019) Rapid Capture and Nondestructive Release of Extracellular Vesicles Using Aptamer-Based Magnetic Isolation. *ACS Sens. 4*, 1245−1251.

(132) Park, K. S., Charles, R. C., Ryan, E. T., Weissleder, R., and Lee, H. (2015) Fluorescence Polarization Based Nucleic Acid Testing for Rapid and Cost-Effective Diagnosis of Infectious Disease. *Chem. - Eur. J. 21*, 16359−63.

(133) Nishiyama, K., Takeda, Y., Maeki, M., Ishida, A., Tani, H., Shigemura, K., Hibara, A., Yonezawa, Y., Imai, K., Ogawa, H., and Tokeshi, M. (2020) Rapid Detection of Anti-H5 Avian Influenza Virus Antibody by Fluorescence Polarization Immunoassay Using a Portable Fluorescence Polarization Analyzer. *Sens. Actuators, B 316*, 128160.

(134) Yi, H. (2020) 2019 novel coronavirus is undergoing active recombination. *Clin. Infect. Dis. 71*, 884−887.

(135) Wang, R., Hozumi, Y., Yin, C., and Wei, G. W. (2020) Decoding SARS-CoV-2 Transmission and Evolution and Ramifications for COVID-19 Diagnosis, Vaccine, and Medicine. *J. Chem. Inf. Model.*, DOI: 10.1021/acs.jcim.0c00501.

(136) Ugurel, O. M., Ata, O., and Turgut-Balik, D. (2020) An updated analysis of variations in SARS-CoV-2 genome. *Turk. J. Biol. 44*, 157−167.

(137) Álvarez-Díaz, D. A., Franco-Muñoz, C., Laiton-Donato, K., Usme-Ciro, J. A., Franco-Sierra, N. D., Flórez-Sánchez, A. C., Gómez-Rangel, S., Rodríguez-Calderon, L. D., Barbosa-Ramirez, J., Ospitia-Baez, E., Walteros, D. M., Ospina-Martinez, M. L., and Mercado-Reyes, M. (2020) Molecular analysis of several in-house rRT-PCR protocols for SARS-CoV-2 detection in the context of genetic variability of the virus in Colombia. *Infect., Genet. Evol. 84*, 104390.

(138) Peñarrubia, L., Ruiz, M., Porco, R., Rao, S. N., Juanola-Falgarona, M., Manissero, D., López-Fontanals, M., and Pareja, J. (2020) Multiple assays in a real-time RT-PCR SARS-CoV-2 panel can mitigate the risk of loss of sensitivity by new genomic variants during the COVID-19 outbreak. *Int. J. Infect. Dis. 97*, 225−229.

(139) Fries, L., Shinde, V., Stoddard, J. J., Thomas, D. N., Kpamegan, E., Lu, H., Smith, G., Hickman, S. P., Piedra, P., and Glenn, G. M. (2017) Immunogenicity and Safety of a Respiratory Syncytial Virus Fusion Protein (RSV F) Nanoparticle Vaccine in Older Adults. *Immun. Ageing 14*, 8.

(140) Sheahan, T. P., Sims, A. C., Zhou, S., Graham, R. L., Pruijssers, A. J., Agostini, M. L., Leist, S. R., Schafer, A., Dinnon, K. H., Stevens, L. J., Chappell, J. D., Lu, X., Hughes, T. M., George, A. S., Hill, C. S., Montgomery, S. A., Brown, A. J., Bluemling, G. R., Natchus, M. G., Saindane, M., Kolykhalov, A. A., Painter, G., Harcourt, J., Tamin, A., Thornburg, N. J., Swanstrom, R., Denison, M. R., and Baric, R. S. (2020) An Orally Bioavailable Broad-Spectrum Antiviral Inhibits SARS-CoV-2 in Human Airway Epithelial Cell Cultures and Multiple Coronaviruses in Mice. *Sci. Transl. Med. 12*, eabb5883.

(141) Gordon, D. E., Jang, G. M., Bouhaddou, M., Xu, J., Obernier, K., White, K. M., O'Meara, M. J., Rezelj, V. V., Guo, J. Z., Swaney, D. L., Tummino, T. A., Huettenhain, R., Kaake, R. M., Richards, A. L., Tutuncuoglu, B., Foussard, H., Batra, J., Haas, K., Modak, M., Kim, M., Haas, P., Polacco, B. J., Braberg, H., Fabius, J. M., Eckhardt, M., Soucheray, M., Bennett, M. J., Cakir, M., McGregor, M. J., Li, Q., Meyer, B., Roesch, F., Vallet, T., Mac Kain, A., Miorin, L., Moreno, E., Naing, Z. Z. C., Zhou, Y., Peng, S., Shi, Y., Zhang, Z., Shen, W., Kirby, I. T., Melnyk, J. E., Chorba, J. S., Lou, K., Dai, S. A., Barrio-Hernandez, I., Memon, D., Hernandez-Armenta, C., Lyu, J., Mathy, C. J. P., Perica, T., Pilla, K. B., Ganesan, S. J., Saltzberg, D. J., Rakesh, R., Liu, X., Rosenthal, S. B., Calviello, L., Venkataramanan, S., Liboy-Lugo, J., Lin, Y., Huang, X. P., Liu, Y., Wankowicz, S. A., Bohn, M., Safari, M., Ugur, F. S., Koh, C., Savar, N. S., Tran, Q. D., Shengjuler, D., Fletcher, S. J., O'Neal, M. C., Cai, Y., Chang, J. C. J., Broadhurst, D. J., Klippsten, S., Sharp, P. P., Wenzell, N. A., Kuzuoglu, D., Wang, H. Y., Trenker, R., Young, J. M., Cavero, D. A., Hiatt, J., Roth, T. L., Rathore, U., Subramanian, A., Noack, J., Hubert, M., Stroud, R. M., Frankel, A. D., Rosenberg, O. S., Verba, K. A., Agard, D. A., Ott, M., Emerman, M., Jura, N., von Zastrow, M., Verdin, E., Ashworth, A., Schwartz, O., d'Enfert, C., Mukherjee, S., Jacobson, M., Malik, H. S., Fujimori, D. G., Ideker, T., Craik, C. S., Floor, S. N., Fraser, J. S., Gross, J. D., Sali, A., Roth, B. L., Ruggero, D., Taunton, J., Kortemme, T., Beltrao, P., Vignuzzi, M., Garcia-Sastre, A., Shokat, K. M., Shoichet, B. K., and Krogan, N. J. (2020) A SARS-CoV-2 Protein Interaction Map Reveals Targets for Drug Repurposing. *Nature 583*, 459.

(142) Tai, W., He, L., Zhang, X., Pu, J., Voronin, D., Jiang, S., Zhou, Y., and Du, L. (2020) Characterization of the Receptor-Binding Domain (RBD) of 2019 Novel Coronavirus: Implication For Development of RBD Protein as a Viral Attachment Inhibitor and Vaccine. *Cell. Mol. Immunol. 17*, 613−620.

(143) Dai, W., Zhang, B., Su, H., Li, J., Zhao, Y., Xie, X., Jin, Z., Liu, F., Li, C., Li, Y., Bai, F., Wang, H., Cheng, X., Cen, X., Hu, S., Yang,

X., Wang, J., Liu, X., Xiao, G., Jiang, H., Rao, Z., Zhang, L. K., Xu, Y., Yang, H., and Liu, H. (2020) Structure-Based Design of Antiviral Drug CandidatesTargeting the SARS-CoV-2 Main Protease. *Science 368*, 1331.

(144) Zhang, L., Lin, D., Sun, X., Curth, U., Drosten, C., Sauerhering, L., Becker, S., Rox, K., and Hilgenfeld, R. (2020) Crystal Structure of SARS-CoV-2 Main Protease Provides a Basis for Design of Improved Alpha-Ketoamide Inhibitors. *Science 368*, 409−412.

(145) Abbott, T. R., Dhamdhere, G., Liu, Y., Lin, X., Goudy, L., Zeng, L., Chemparathy, A., Chmura, S., Heaton, N. S., Debs, R., Pande, T., Endy, D., La Russa, M. F., Lewis, D. B., and Qi, L. S. (2020) Development of CRISPR as an Antiviral Strategy to Combat SARS-CoV-2 and Influenza. *Cell 181*, 865−876.

(146) Zhang, J., Litvinova, M., Liang, Y., Wang, Y., Wang, W., Zhao, S., Wu, Q., Merler, S., Viboud, C., Vespignani, A., Ajelli, M., and Yu, H. (2020) Changes in Contact Patterns Shape the Dynamics of the COVID-19 Outbreak in China. *Science 368*, 1481−1486.

(147) Corman, V. M., Landt, O., Kaiser, M., Molenkamp, R., Meijer, A., Chu, D. K., Bleicker, T., Brünink, S., Schneider, J., Schmidt, M. L., et al. (2020) Detection of 2019 Novel Coronavirus (2019-nCoV) by Real-Time RT-PCR. *Euro. Surveill. 25*, 2000045.

(148) Chan, J. F.-W., Yip, C. C.-Y., To, K. K.-W., Tang, T. H.-C., Wong, S. C.-Y., Leung, K.-H., Fung, A. Y.-F., Ng, A. C.-K., Zou, Z., Tsoi, H.-W., et al. (2020) Improved Molecular Diagnosis of COVID-19 by the Novel, Highly Sensitive and Specific COVID-19-RdRp/Hel Real-Time Reverse Transcription-Polymerase Chain Reaction Assay Validated in Vitro and with Clinical Specimens. *J. Clin. Microbiol. 58*, e00310-20.

(149) Chu, D. K. W., Pan, Y., Cheng, S. M. S., Hui, K. P. Y., Krishnan, P., Liu, Y., Ng, D. Y. M., Wan, C. K. C., Yang, P., Wang, Q., Peiris, M., and Poon, L. L. M. (2020) Molecular Diagnosis of a Novel Coronavirus (2019-nCoV) Causing an Outbreak of Pneumonia. *Clin. Chem. 66*, 549−555.

(150) Lamb, L. E., Bartolone, S. N., Ward, E., and Chancellor, M. B. (2020) Rapid Detection of Novel Coronavirus (COVID19) by Reverse Transcription-Loop-Mediated Isothermal Amplification. *PLoS One 15*, No. e0234682.

(151) Moitra, P., Alafeef, M., Dighe, K., Frieman, M., and Pan, D. (2020) Selective Naked-Eye Detection of SARS-CoV-2 Mediated by N Gene Targeted Antisense Oligonucleotide Capped Plasmonic Nanoparticles. *ACS Nano 14*, 7617.

(152) Qiu, G., Gai, Z., Tao, Y., Schmitt, J., Kullak-Ublick, G. A., and Wang, J. (2020) Dual-Functional Plasmonic Photothermal Biosensors for Highly Accurate Severe Acute Respiratory Syndrome Coronavirus 2 Detection. *ACS Nano 14*, 5268−5277.

https://dx.doi.org/10.1021/acsinfecdis.0c00365
ACS Infect. Dis. 2020, 6, 1998−2016